



Physiological and Proteomic Changes in the Apoplast Accompany Leaf Senescence in *Arabidopsis*

Maria L. Borniego, Maria C. Molina, Juan J. Guiamét and Dana E. Martinez*

Instituto de Fisiología Vegetal (INFIVE), CONICET-Universidad Nacional de La Plata, La Plata, Argentina

OPEN ACCESS

Edited by:

Judy Brusslan,
California State University, Long Beach,
United States

Reviewed by:

Christine Helen Foyer,
University of Leeds,
United Kingdom
Klaus Humbeck,
Martin Luther University
of Halle-Wittenberg, Germany

*Correspondence:

Dana E. Martinez
danamartinez@conicet.gov.ar

Specialty section:

This article was submitted to
Plant Physiology,
a section of the journal
Frontiers in Plant Science

Received: 03 June 2019

Accepted: 20 November 2019

Published: 08 January 2020

Citation:

Borniego ML, Molina MC, Guiamét JJ
and Martinez DE (2020) Physiological
and Proteomic Changes in the
Apoplast Accompany Leaf
Senescence in *Arabidopsis*.
Front. Plant Sci. 10:1635.
doi: 10.3389/fpls.2019.01635

The apoplast, i.e. the cellular compartment external to the plasma membrane, undergoes important changes during senescence. Apoplastic fluid volume increases quite significantly in senescing leaves, thereby diluting its contents. Its pH elevates by about 0.8 units, similar to the apoplast alkalization in response to abiotic stresses. The levels of 159 proteins decrease, whereas 24 proteins increase in relative abundance in the apoplast of senescing leaves. Around half of the apoplastic proteins of non-senescent leaves contain a N-terminal signal peptide for secretion, while all the identified senescence-associated apoplastic proteins contain the signal peptide. Several of the apoplastic proteins that accumulate during senescence also accumulate in stress responses, suggesting that the apoplast may constitute a compartment where developmental and stress-related programs overlap. Other senescence-related apoplastic proteins are involved in cell wall modifications, proteolysis, carbohydrate, ROS and amino acid metabolism, signaling, lipid transport, etc. The most abundant senescence-associated apoplastic proteins, PR2 and PR5 (e.g. pathogenesis related proteins PR2 and PR5) are related to leaf aging rather than to the chloroplast degradation program, as their levels increase only in leaves undergoing developmental senescence, but not in dark-induced senescent leaves. Changes in the apoplastic space may be relevant for signaling and molecular trafficking underlying senescence.

Keywords: apoplast, senescence, apoplastic fluid, secretome, extracellular pH, pathogenesis-related protein, PR

INTRODUCTION

At the leaf level, senescence represents a degenerative process, but, at the same time it constitutes an efficient nutrient recycling mechanism for the plant. Most of the nitrogen released from senescing leaves comes from Rubisco and other plastid proteins degradation; therefore a major focus of senescence research has been to elucidate the mechanism for chloroplast dismantling (Noodén et al., 1997; Guiamet et al., 2002; Otegui, 2018). Other cellular changes occurring in senescing leaves are less characterized, and even less is known about the adjustments taking place outside the plasma membrane as leaf senescence progresses.

Abbreviations: AF, apoplastic fluid; AWF, apoplastic wash fluid; AFS2–AFS3, apoplastic fluid protein pattern from S2 and S3 leaves, respectively; AFSP, apoplastic fluid senescence-related protein.

The apoplast is the space external to the plasma membrane that includes cell walls, middle lamella, intercellular spaces, and the fluid that moves freely within the walls and intercellular spaces, known as extracellular fluid or apoplastic fluid (AF). The AF represents around 4% to 11% of the total leaf fresh weight (Sattelmacher and Horst, 2007). Its composition consists of molecules related to metabolism and signaling, such as amino acids, polysaccharides, secondary metabolites, ions, and secreted mRNA and proteins with several functions, particularly enzymes related to defense and proteolysis (Sattelmacher and Horst, 2007; Martínez-González et al., 2018). The apoplast plays a critical role in plant development, as it provides the environment for cell expansion and cell wall maintenance, ion and molecule trafficking, source-to-sink translocation of nutrients, intercellular and systemic signaling, stress perception, and response (Hoson, 1998; O'Leary et al., 2016; Rodríguez-Celma et al., 2016). Stress-elicited changes in the apoplast have been extensively examined, and these include modulation of the pH and fine tuning of protein abundance and composition (Felle, 2001; Dani et al., 2005; Floerl et al., 2012; Geilfus, 2017). Apoplastic pH (pH_{apo}) transiently increased under drought and salinity becoming more alkaline as the stresses intensify (Geilfus et al., 2015; Zörb et al., 2015; Geilfus, 2017). Also, pathogen and peptide signals, such as systemin and RALF (rapid alkalization factor), trigger apoplast alkalization (Felle et al., 2004; Higgins et al., 2007; Masachis et al., 2016). The pH_{apo} varies along ontogeny (Mattsson and Schjoerring, 2003; Wu et al., 2016), and along with pH_{apo} , the extracellular space volume might adjust as the leaf ages (Husted and Schjoerring, 1995; Lohaus et al., 2001; Nouchi et al., 2012). Apoplast conditions influence chloroplast metabolism and leaf physiology (Karpinska et al., 2018) and therefore might influence senescence-related processes, for instance the regulation of intra to extracellular exchange of molecules and long distance remobilization of nutrients. Transcription analysis of *Arabidopsis* plasma membrane transporters suggest that molecule trafficking across the plasma membrane might increase during leaf senescence (Van Der Graaff et al., 2006).

Proteomic approaches identified chitinases, pathogenesis related proteins (PR), and other defense related enzymes, as the mayor leaf apoplastic proteins (Boudart et al., 2005; Rutter and Innes, 2017; Soares et al., 2017). The extracellular accumulation of these enzymes along with the transient alkalization of pH_{apo} as signature of different biotic and abiotic stress responses suggest either a cross-talk between stress pathways or a common apoplastic signal-transducing element or node (Geilfus, 2017).

Many of the stress-related extracellular enzymes are constitutive members in the AF that activate and/or accumulate upon specific signals, some of them are also up-regulated during senescence (Grudkowska and Zagdanska, 2004; Goulet et al., 2010). Other stress-related enzymes relocate inside/outside the cell in response to external stimulus. Caspase-like serine proteases from *Avena sativa* relocate from the cytosol to the apoplast upon programmed cell death (PCD) induction (Coffeen and Wolpert, 2004), whereas some apoplastic subtilisin proteases re-enter cells committed to PCD (Trusova et al., 2019).

Similar intra-extracellular pathways might be involved in the regulation and/or execution of leaf senescence.

Compared to stress-related broad analysis of AF proteomes (Kosová et al., 2011; Gupta et al., 2015), there is not enough information on the AF proteome dynamics in senescing leaves, however different studies evidence relevant roles for apoplastic proteins during this leaf stage. By regulating long-distance movement of sucrose, the extracellular invertase (cwINV) and its inhibitor (INVINH) probably play a crucial role in the regulation of senescence by controlling source-sink relations (Lara et al., 2004; Jin et al., 2009). The apoplastic subtilisin protease SASP is highly up-regulated during senescence, and whereas *at-sasp* plants do not differ from wild type plants at vegetative stage, they produce more branched inflorescences, siliques, and seeds (Martinez et al., 2015). The *Arabidopsis* extracellular metalloprotease At2-MMP is up-regulated as the plant ages, and *at2-mmp-1* plants show accelerated chlorophyll (Chl) degradation and delayed flowering (Delorme et al., 2000; Gollmack et al., 2002). Other apoplastic proteases from different mechanistic classes (cysteine-, metallo-, and serine- proteases) are up-regulated during leaf senescence (Martínez and Guíamet, 2014).

This study aimed to shed light on the dynamics of the extracellular space during leaf senescence by analyzing physiological parameters of the apoplast space and the AF, including a large-scale quantitative proteomic approach to compare the AF proteomes of senescent and non-senescent leaves.

MATERIALS AND METHODS

Plant Material and Growth Conditions

Arabidopsis thaliana Col-0, wild type, and the transgenic line apo-pHusion (Gjetting et al., 2012) were used. Apo-pHusion plants express the chimeric apo-mRFP1-EGFP protein targeted to the apoplast, where it functions as a pH sensor (Gjetting et al., 2012). The plants were cultivated in 550 mL pots filled with soil and vermiculite (2:1 v/v). Nitrofoska[®] was applied (30 mL, 1 g/L per pot) every 30 days. The plants were grown in growth chambers, at 24°C and 120 $\mu\text{mol m}^{-2} \text{s}^{-1}$ photosynthetic photon flux density under a 10 h light/14 h dark photoperiod.

Each rosette was separated in groups of leaves based on the phyllotaxis and leaf size. Vegetative rosettes were separated in two groups of leaves, the youngest named S1 (Stage 1), whereas rosettes at reproductive stages were separated in three, four, or five groups of leaves, according to the rosette age and leaf number (stages S2, S3, and S4). Around six to eight consecutive leaves representing one stage (S1, 2, 3, or 4) were sampled per plant. Each plant was harvested only once and for one particular Stage only.

Physiological Parameters

Leaf chlorophyll content was measured non-destructively with the SPAD 502 Portable Chlorophyll Meter (Konica-Minolta[®]).

Maximum quantum yield of photosystem II (Fv/Fm) measurements were taken with a modulated pulse fluorimeter FMS 2 (Hansatech[®]). The leaves were acclimated for 30 min in the dark before the measurements.

Leaf water content, LWC, was determined as:

$$LWC = [(FW - DW)/FW] \times 100$$

Relative water content, RWC, was determined as:

$$RWC = [(FW - DW)/(SW - DW)] \times 100$$

where FW = fresh weight, DW = dry weight, SW = water saturated weight.

Water potential (Ψ_w) of 5 mm diameter leaf discs was measured with a dew point psychrometer and C-52 chambers (Wescor®). Sodium chloride solutions of different concentrations were absorbed in filter paper discs and used for calibration.

Solute potential (Ψ_s): measurements were carried out in a vapor pressure micro osmometer Vapro 5520 (Wescor®), using 10 μ L per sample. To measure leaf Ψ_s , leaves without the midrib were frozen in liquid nitrogen and placed in a 1 mL syringe containing glass wool at the bottom. Pressure was applied pushing the plunger and the resulting leaf macerates were analyzed. The Ψ_s of the AF was estimated measuring the Ψ_s of the apoplastic wash fluids (AWFs), and correcting the obtained values by their corresponding dilution factors (F_{dil}) (See below).

Leaf AWF Extraction

Leaf infiltration was performed with cold deionized water using a 60 mL syringe as described in O'Leary et al. (2014). Infiltrated leaves were stuck, with petioles facing up into a 50-mL centrifuge tube and centrifuged at 600 g for 40 min at 4°C. For protein analysis, 5 μ L of 300 mM phenylmethylsulfonyl fluoride (PMSF) was added at the bottom of the tube prior to centrifugation.

Estimation of the Apoplast Volume Occupied by Fluid (V_{AF}) and Air (V_{air}) and of AWF Dilution Factor

Estimations of V_{air} and V_{AF} were carried out by the Indigo Carmine (indigo-5.5'-disulfonic acid, disodium salt, IC) method (Husted and Schjoerring, 1995) with modifications. Fully hydrated leaves were excised from *Arabidopsis* plants, weighed, and vacuum infiltrated, as described above, but with 50 μ M IC, in 10 mM sodium phosphate buffer pH 6.2. Once infiltrated, leaf surfaces were blotted, immediately re-weighed, and centrifuged. The difference in the leaf weight before and after infiltration (corrected by the density of IC solution) was used for calculation of the apoplastic air volume (V_{air}) (Lohaus et al., 2001).

The IC infiltration solution and AWFs were measured spectrophotometrically at 610 nm to calculate the IC concentration. The volume of AF (V_{AF}) was calculated using the following equation:

$$V_{AF} = (V_{air} \times Abs_{610}IC) / Abs_{610}AWF - V_{air}$$

The dilution factor (F_{dil}) of AWF was calculated based on V_{AF} and V_{air} :

$$F_{dil} = (V_{AF} + V_{air}) / V_{AF}$$

The physiological concentration of solutes and metabolites in the AF was calculated by multiplying the solute or metabolite concentration in the AWF by its dilution factor, F_{dil} .

Cytoplasmic Contamination in Apoplast Fluids

The cytosolic marker glucose-6-phosphate dehydrogenase (G6PDH, EC 1.1.1.49) was assayed at room temperature in 100 μ L 100 mM Tris-HCl pH 8, 6.7 mM MgCl₂, 12 mM glucose-6-P, 0.4 mM NADP⁺ and AWF or leaf extracts. NADP⁺ reduction was followed at 340 nm. Leaf extracts were obtained by homogenizing leaves at 4°C in 100 mM Tris-HCl pH 8, 4 mM PMSF; and centrifuging for 15 min at 15,000 g, 4°C.

In Vivo Estimation of Leaf Apoplast pH by Confocal Fluorescence Microscopy

Ex Vivo Calibration of pHusion

Aliquots of AWF extracted from apo-pHusion plants were incubated with 300 mM Tris-HCl or 300 mM MES buffers adjusted with HCl or KOH to different pH values, placed in microscope slides with cavities, and detected by confocal microscopy. Confocal data acquisition was performed with a Leica TCS SP5 II CLSM with the following setting: Ex 488/Em 524–550 nm for EGFP, and Ex 543/Em 566–634 nm for mRFP1. For each pH value, pixel intensity of the fluorescence ratio EGFP/mRFP1 in a region of interest (ROI) was calculated using the software ImageJ. A non-linear fitting of average pixel intensities was calculated using ImageJ software, and the software GraphPad Prism was used to generate a sigmoid curve.

In Vivo Observation of Apoplastic Apo-pHusion

Images of apo-pHusion S2 and S3 leaves were acquired by confocal microscopy, with the setting described above. Ratio images EGFP/mRFP1 were generated using the software ImageJ and the average pixel intensities EGFP/mRFP1 for each ROI were calculated. PH values were estimated by extrapolation on the calibration curve. LAS AF software version 2.2.1 was used for image acquisition. For visual presentation of ratio images, a pseudocolor look-up table was designed using the software ImageJ.

Isolation of Cell Wall Polysaccharides and Cell Wall Quantitation

Cell wall polysaccharides were obtained from alcohol insoluble residues (AIR) according to Nardi et al. (2015). To estimate the amount of cell wall, the starch was subtracted from each AIR with Dimethyl sulfoxide (DMSO) according to Carpita and Kanabus (1987). After removing the starch, the resulting AIR was incubated with 0.01 M HCl in a boiling water bath for 2 h and filtered for polyuronide extraction. The obtained solution was used for pectin quantification (see below).

Hydrolysis and Quantification of Pectins

100 μ L of the polyuronide filtrate was mixed with 600 μ L of 0.0125 M sodium tetraborate in saturated H₂SO₄, incubated in a

water bath for 20 min. and cooled down. Uronic acid concentrations were estimated by the m-hydroxydiphenyl method (Blumenkrantz and Asboe-Hansen, 1973) using galacturonic acid as standard.

Starch Quantification

Around 0.1 mL of DMSO extract was mixed with 1 mL of 0.05% w/v anthrone in 66% v/v H₂SO₄ and incubated at 100°C for 10 min and cooled down. The starch content was measured spectrophotometrically at 620 nm using glucose as standard.

Transmission Electron Microscopy

Around 2 mm² pieces were sectioned from the middle region of the leaf and fixed by immersion in 2% glutaraldehyde, post fixed in 1% osmium tetroxide and dehydrated through a graded series of ethanol and embedded in epoxy resin. Ultrathin sections were cut with a Super Nova Reichert–Jung Ultra-microtome (Wien Austria), and examined with a JEM 1200 EX II transmission electron microscope (JEOL Ltd., Tokio, Japan). Cell wall analysis was performed with Image J software on at least three different leaves of each stage.

Protein Analysis

Leaves were homogenized in 50 mM Tris-HCl pH 8, 20 mM ethylenediaminetetraacetic acid (EDTA), 10 mM PMSF and 1% insoluble polyvinylpyrrolidone, and cleared at 15,000 g, 4°C for 15 min. Laemmli's Sample Buffer, LSB, was added before electrophoresis. Aliquots of AWF were lyophilized in a vacuum freeze-dryer (Scientz®-10 N) and the pellets were re-suspended in LSB.

SDS-PAGE gels (12% w/v acrylamide) were run in a Mini-PROTEAN® III cell (Bio-Rad), and stained with Coomassie Brilliant Blue R-250 (CBB) or with Coomassie Blue Colloidal G-250 (G-250).

Densitometric quantification of protein bands in CBB-stained gels was performed by using the ImageJ 1.6 software (National Institutes of Health, USA).

Peptide and Protein Quantification

The Pierce® BCA Protein Assay Kit (Thermo Scientific) using bovine serum albumin as standard was used with AWFs and leaf extracts

Western Blot and Immunodetection

SDS-PAGE gels were transferred to nitrocellulose membranes using a Bio Rad Miniprotean System. The membrane was blocked with 10% milk in PBST buffer, incubated with a polyclonal antibody against Rubisco Large Subunit, and developed with a horseradish peroxidase-conjugated secondary antibody.

Protein Identification and Quantification by LC-MS/MS and Bioinformatics

For the identification of proteins in SDS-PAGE gels the bands were excised from G-250 stained gels, washed, dried, reduced, alkylated, and trypsin digested. Peptides were extracted with three steps of 50% acetonitrile/0.5% trifluoroacetic acid, and

desalted with a Zip-Tip C18. Samples were analyzed by LC-MSMS using a Q Exactive™ nano HPLC-ESI-Orbitrap mass spectrometer (Thermo Fisher Scientific). Protein identification was performed with Proteome Discoverer 1.4 (Thermo Fisher Scientific) connected to a Mascot search engine server (Matrix Science, London, UK). Only proteins identified with at least two unique peptides with 0.99 confidence (FDR = 0.01) were considered.

For large-scale protein analysis by shotgun proteomics, lyophilized AWF aliquots were resuspended in 8 M urea; aliquots containing 20 µg of protein were reduced, alkylated, trypsin digested, and desalted. LC-MSMS analysis was performed as described previously. A *label-free-quantification* method was performed using Proteome Discoverer 1.4. Four biological replicates for each leaf stage were analyzed. Identified proteins were submitted to a Student's t-test ($P \leq 0.05$) with Perseus 1.6.1.3 (Max Planck Institute of Biochemistry). Only proteins exhibiting at least a $\pm 100\%$ fold change in their amount were considered.

Statistical Analysis

Data from parameters (Chl, protein content) were tested either with one-way ANOVA and Tukey tests ($P \leq 0.05$), with two-way ANOVA and Holm-Sidak test ($p \leq 0.05$), or with Dunnett's multiple comparisons test. For paired analysis of S2 and S3 leaf stages, means were compared using the Student's t-test ($p \leq 0.05$). Statistical analysis was plotted using the GraphPad Prism 6.01 software (GraphPad Software, San Diego, CA, USA). The number of independent replicates, i.e, biological samples (n), and the corresponding technical replicates are indicated in each table and figure caption.

Cell wall thickness was analyzed by one-way ANOVA, and univariate tests of significance, Sigma-restricted parameterization Effective hypothesis decomposition ($P \leq 0.0001$).

RESULTS AND DISCUSSION

Leaf Developmental Stages and Apoplastic Fluid Isolation

In order to characterize changes in the apoplast accompanying senescence, leaf developmental stages were defined and apoplast fluids (AFs) were isolated. Four leaf stages were characterized: non-senescent leaves from plants at vegetative (S1) and early reproductive stages (S2), and senescing leaves from plants at mid (S3) and late reproductive stages (S4) (**Figures 1A, B**). Chl and protein content per leaf area and Photosystem II maximum photochemical efficiency (Fv/Fm) were determined. S1 and S2 leaves showed no difference in Rubisco and total leaf protein content (**Figure 1C**), PSII integrity, as assessed by Fv/Fm, (**Figure 1E**), and S2 Chl concentration was slightly higher than in S1 leaves (**Figure 1D**). S3 and S4 leaves showed clear signs of senescence, i.e. Chl and protein levels and Fv/Fm decreased in S3 and S4 compared to S1 and S2. Particularly, the amount of leaf protein dropped down to 40 and 20% in S3 and S4 respectively, compared to non-senescent S1 and S2 leaves. AF isolation was performed

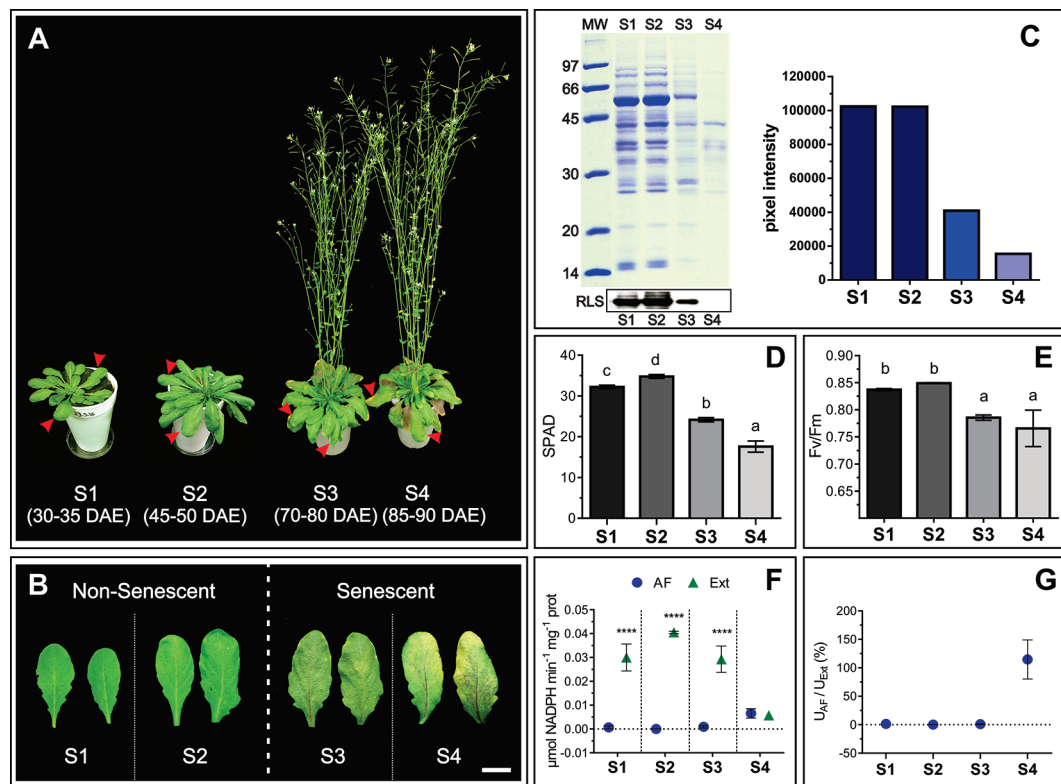


FIGURE 1 | Physiological characteristics of S1, S2, S3, and S4 leaves. **(A)** Leaf stages, marked with red arrows, DAE: Days after emergence. **(B)** Mature, non-senescent leaves (S1 and S2) and senescent leaves (S3 and S4), scale bar 2 cm. **(C)** Leaf protein content: Representative SDS-PAGE showing a total protein profile loaded per unit leaf area, and immunodetection of Rubisco Large Subunit (RLS), in the left upper and lower panel, respectively. Relative leaf protein content, considering S1 as maximum, was estimated by densitometric analysis of the SDS-PAGE, and it is shown on the right panel. **(D)** Chlorophyll content per unit leaf area expressed in SPAD units. **(E)** Maximum quantum yield of Photosystem II (Fv/Fm). **(F)** Enzymatic activity (U) of the cytosolic enzyme G6PDH in apoplastic fluid (AF) and total leaf extracts (Ext) expressed on the basis of total protein (prot) content. **(G)** Percentage of G6PDH activity in AF as a function of G6PDH activity in Ext. Values in the graphs show the average \pm standard error, SEM, of independent measurements. Data were normally distributed. SPAD readings were taken in 10 to 15 different leaves for each stage, two readings per leaf blade. Fv/Fm values are the average of 16 leaves (S1), 30 leaves (S2 and S3), and six different S4 leaves, one reading per leaf blade. G6PDH activity **(D and E)** represents the average of biological samples (n), where each FA and Ext biological sample was made up of at least 4 leaves. S1: n = 6 FA and Ext n = 6, S2: n = 4 FA and n = 3 Ext, S3: n = 9 FA and n = 5 Ext, S4: n = 3 FA and 3 Ext. Significant differences were calculated at $P \leq 0.05$ between the conditions using the Tukey test; letters indicate significant differences between stages. Asterisks indicate significant differences between AF and Ext; ****, $P < 0.0001$, calculated using a two-way ANOVA test.

following the vacuum infiltration–centrifugation method (Lohaus et al., 2001; O’Leary et al., 2014) and obtained AF fractions (from here on AWFs) were tested for potential contamination with intracellular compounds. AWFs and whole leaf extracts were assayed for the cytosol marker Glucose 6P Dehydrogenase (G6PDH), which was expressed as G6PDH activity in AWF as a percentage of the whole leaf extract activity (Figures 1F, G). AWF from S1 to S3 leaves were devoid of detectable G6PDH activity, whereas AWF S4 showed high activity of the cytosolic enzyme, indicating the presence of intracellular compounds in the AWF, probably due to age-related loss of cell membrane integrity (Figure 1G). Based on whole-leaf and AWF analysis (Figures 1A–G), S3 leaves show clear signs of senescence while still retaining cell integrity, whereas S4 leaves would represent the culmination of the remobilization process followed by membrane permeabilization and cell death. S1 and S2 showed no difference in senescence-related parameters; therefore S2 was selected as non

senescent leaf stage to compare its apoplastic space and AF with that of senescing S3 leaves. Both S2 and S3 leaves belong to plants at reproductive stage and that would avoid or minimize any variation in the apoplast related to different phases of plant development.

Water Relations of Non Senescing and Senescing Leaves. Relative Water Content and Water Potential in S2 and S3 Leaf Stages

Leaf water status directly affects the apoplast water content and therefore its metabolite concentration (Tyree, 1976; Andersen et al., 1991; Wardlaw, 2005). Water relations vary throughout *Arabidopsis* leaf development, particularly right after the leaf reaches its maximum extension and starts yellowing (Breeze et al., 2011). Relative water content (RWC), moisture, and water

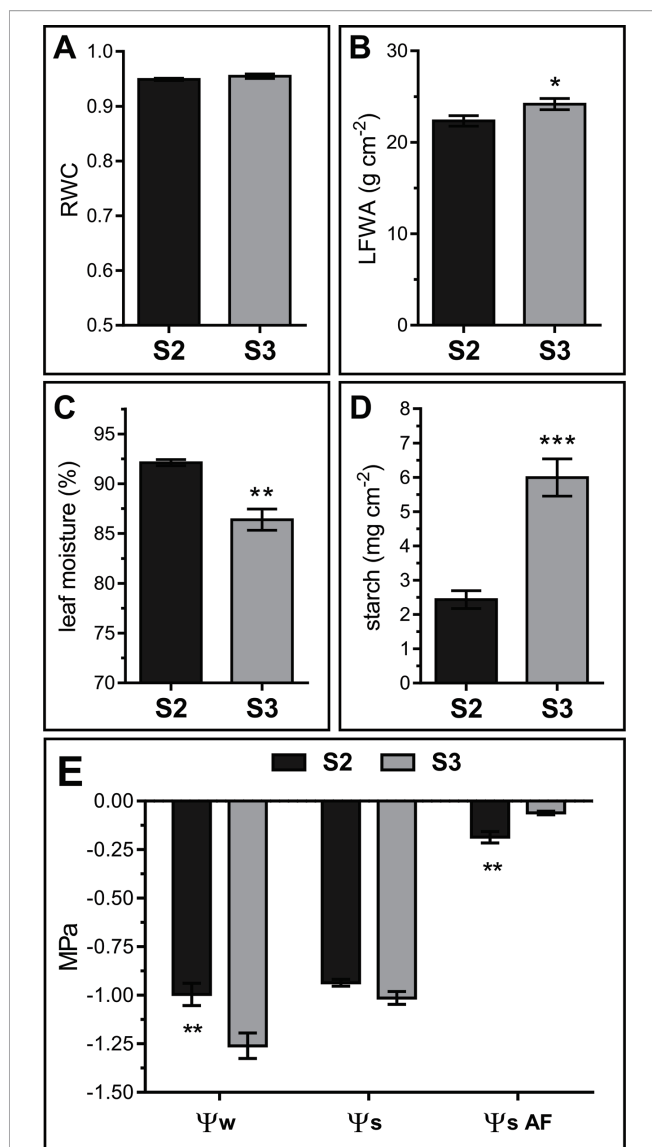


FIGURE 2 | Water relations in S2 and S3 leaves. **(A)** Relative water content (RWC). **(B)** Leaf fresh weight per unit of leaf area (LFWA). **(C)** Leaf water content (LWC), expressed as percentage of water per leaf FW. **(D)** Starch content expressed as mg of glucose per unit leaf area. **(E)** Leaf water potential (Ψ_w) measured on leaf disks, solute potential of freeze-thaw squeezed leaves (Ψ_s) and AF solute potential ($\Psi_{s\ AF}$). Data represents the average of biological samples (n). **(A)** RWC: n = 6 (S2) and n = 6 (S3), **(B)** LFWA: n = 11 (S2) and n = 13 (S3), **(C)** LWC: n = 6 (S2) and n = 6 (S3), **(D)** starch: n = 5 (S2) and n = 6 (S3), **(E)** Ψ_w : n = 13 (S2) and n = 13 (S3), Ψ_s : n = 4 (S2) and n = 6 (S3), $\Psi_{s\ AF}$: n = 4 (S2) and n = 4 (S3). Values were normally distributed and significant differences were calculated between S2 and S3 at $P \leq 0.05$ using the Student's t test: *, $P < 0.05$; **, $P < 0.01$; ***, $P < 0.001$. Values in the graphs show the average \pm SEM.

potential (Ψ_w) were determined in S2 and S3 leaves. RWC remained constant between S2 and S3 stages (S2 RWC = 0.949 ± 0.002 and S3 RWC = 0.955 ± 0.004) (Figure 2A). However, percentage leaf water content decreased and leaf fresh weight per area (LFWA) increased in S3 compared to S2 leaves (Figures 2B, C). A higher LFWA might relate to starch

accumulation during senescence (Oda-Yamamizo et al., 2016). The 3-fold increase in starch content detected from S2 to S3 leaves (Figure 2D) might explain the higher LFWA in S3 leaves.

Leaf water potential dropped from S2 to S3 ($\Psi_w = -1.00 \pm 0.21$ to -1.26 ± 0.25 MPa, respectively), whereas the solute potential remained stable between stages (Ψ_s S2 = -0.94 ± 0.03 and Ψ_s S3 = -1.01 ± 0.08) (Figure 2E, left and middle parts of the graph). Intriguingly, experimental Ψ_s values were the same or higher than Ψ_w values. Since extracts from frozen-thawed squeezed leaves are composed of cellular, AF and xylem contents, it would be plausible that AF and xylem fluids diluted the cellular sap, leading to higher Ψ_s than expected based on leaf disk Ψ_w values. Yet, a methodological artifact cannot be dismissed since Ψ_w was measured in fresh leaf disks with a dew point psychrometer, whereas Ψ_s was measured in frozen-squeezed leaves using a vapor pressure micro-osmometer.

S2 and S3 AF solute potential ($\Psi_{s\ AF}$) was estimated measuring AWFs with the vapor pressure microosmometer, and correcting the obtained AWF Ψ_s values by the corresponding dilution factor (see Materials and Methods, Leaf AWF Extraction). Estimated apoplastic $\Psi_{s\ AF}$ was significantly higher than leaf Ψ_s , and differs between leaf stages; $\Psi_{s\ AF}$ values were higher in S3 with respect to S2, thus evidencing a more diluted AF in senescing leaves (Figure 2E, right side of the graph).

Leaf Senescence-Related Changes in the Apoplast Volume, Apoplastic Air-Fluid Ratio, and Cell Wall Properties

To explore potential changes in the extracellular space volume along leaf senescence the apoplastic air (V_{air}) and AF (V_{AF}) volumes were determined in S2 and S3 leaves (Table 1).

Volume determinations were performed with the Indigo carmine, IC, technique (Husted and Schjoerring, 1995; Lohaus et al., 2001) in multiple independent assays. Determined V_{air} and V_{AF} values were similar to those reported for other species, in the range between 40 and 200 μL per gr of leaf FW (Dietz, 1997; Lohaus et al., 2001; Nouchi et al., 2012). The V_{air} remained stable between S2 and S3 stages, whereas V_{air} was shown to increase with age in *Brassica napus* and *Vicia faba* (Husted and Schjoerring, 1995; Lohaus et al., 2001). When expressed on a leaf fresh weight, LFW, basis there was a slight decrease of 4.6% V_{air} in S3 compared to S2 ($303.50 \pm 4.17 \mu\text{L g}^{-1}$ LFW in S2 and $289.60 \pm 2.05 \mu\text{L g}^{-1}$ LFW in S3) whereas when the V_{air} was expressed per unit leaf area there was no significant difference between S2 and S3. On the other hand, V_{AF} increased significantly as leaves aged. S3 leaves contained 157% more AF than S2 leaves ($21.40 \pm 1.57 \mu\text{L g}^{-1}$ LFW in S2 and $55.01 \pm 1.95 \mu\text{L g}^{-1}$ LFW in S3). When V_{AF} was expressed per unit leaf area S3 leaves showed a 173% increase compared to S2 ($0.49 \pm 0.04 \mu\text{L cm}^{-2}$ and $1.34 \pm 0.04 \mu\text{L cm}^{-2}$ in S2 and S3, respectively). The higher fresh weight per unit area in S3 with respect to S2 leaves (Figure 2B) might explain the differences observed when apoplast volumes (V_{AF} or V_{air}) are expressed on a leaf area or on a LFW basis. The increased V_{AF} in S3 leaves is

TABLE 1 | Apoplastic volumes occupied by fluid (AF) and air in S2 and S3 leaves.

	Apoplastic fluid volume (V_{AF})		Apoplastic air volume (V_{air})		F_{dil}
	$\mu\text{L cm}^{-2}$	$\mu\text{L g}^{-1}$ LFW	$\mu\text{L cm}^{-2}$	$\mu\text{L g}^{-1}$ LFW	
S2	0.49 ± 0.04	21.40 ± 1.57	7.03 ± 0.15	303.50 ± 4.17	18.25 ± 1.38
S3	1.34 ± 0.04 ****	55.01 ± 1.95 ****	7.13 ± 0.11	289.60 ± 2.05 ***	6.54 ± 0.22 ****

Apoplastic volumes were expressed in μL per gram of leaf fresh weight (LFW) and in μL per unit leaf area. Obtained V_{air} and V_{AF} values were used to estimate AWF dilution factor (F_{dil} , see equation in Materials and Methods). Data were normally distributed and significant differences were calculated at $P \leq 0.05$ between leaf stages using the Student's *t* test. Each value represents the mean of 35 to 55 biological samples, *n*, where each sample was made up of at least four leaves. Asterisks indicate significant differences: ***, $P < 0.001$; ****, $P < 0.0001$.

TABLE 2 | Cell wall and pectin content in S2 and S3 leaves.

Leaf	Cell wall		Pectin	
	mg cm^{-2}	mg g^{-1} LFW	mg cm^{-2}	mg g^{-1} LFW
S2	1.09 ± 0.02	48.16 ± 1.00	0.06 ± 0.00	5.06 ± 0.24
S3	1.20 ± 0.09	48.86 ± 2.88	0.08 ± 0.01	6.65 ± 0.54

Values were expressed in mg per gram of leaf fresh weight (LFW) and in mg per unit leaf area. The amount of pectin was expressed as mg of uronic acids. Mean values ± SEM are given. Data were normally distributed and significant differences were calculated at $P \leq 0.05$ between the stages using the Student's *t*-test. Each value represents the mean of biological samples, *n*. S2: *n* = 3, S3: *n* = 4, where each sample was made up of a group of S2 or S3 leaves.

consistent with their higher Ψ_{SAF} (Figure 2G). An age-related increase in V_{AF} was also observed in leaves of *B. napus* and *V. faba* (Husted and Schjoerring, 1995; Lohaus et al., 2001), whereas V_{AF} was reported to decrease during rice leaf senescence (Nouchi et al., 2012). An increase in V_{AF} has also been observed in plants under different types of stress (Rascio et al., 1992; Tetlow and Farrar, 1993; Lohaus et al., 2001; Hamouda et al., 2016).

It has been proposed that cell wall mass and structure, particularly the type and content of pectin polymers that affect the water retention potential of the cell walls (Levesque-Tremblay

et al., 2015) influence the V_{AF} . (Boyer, 1967; Tyree, 1976). We surmised that the steep increase in V_{AF} in S3 leaves would be due to differences in the cell wall properties between leaf stages. To test this hypothesis, the amount of cell wall and pectins, quantified as AIR without starch, and uronic acid concentration, respectively, as well as cell wall thickness were compared between S2 and S3 leaves. Cell wall and pectin content did not differ significantly between S2 and S3, even though there was a slight increase in the pectin content in S3 leaves (Table 2). It has been demonstrated that cell-wall components continue to be deposited into the wall even after the cell no longer expands leading to an increase in cell wall thickness (Wei and Lintilhac, 2007), however the cell wall content is similar in S2 and S3. Interestingly, senescing leaves showed slightly thicker spongy mesophyll cell walls compared to those of non-senescing leaves (247.9 ± 3.0 and 278.8 ± 2.9 nm in S2 and S3, respectively) (Figure 3). Water retained inside the wall might lead to increased thickness (Forouzesh et al., 2013). Also, modifications such as methylesterifications and ion cross-links directly affect the water binding capacity of pectins, and these changes occur in response to abiotic stress and along leaf development (Levesque-Tremblay et al., 2015). Forouzesh et al. (2013) showed that cell wall thickness increases with plant age, and the oldest leaves have thinner walls compared to the newer ones. The results presented here can be reconciled with those of Forouzesh et al. (2013) since

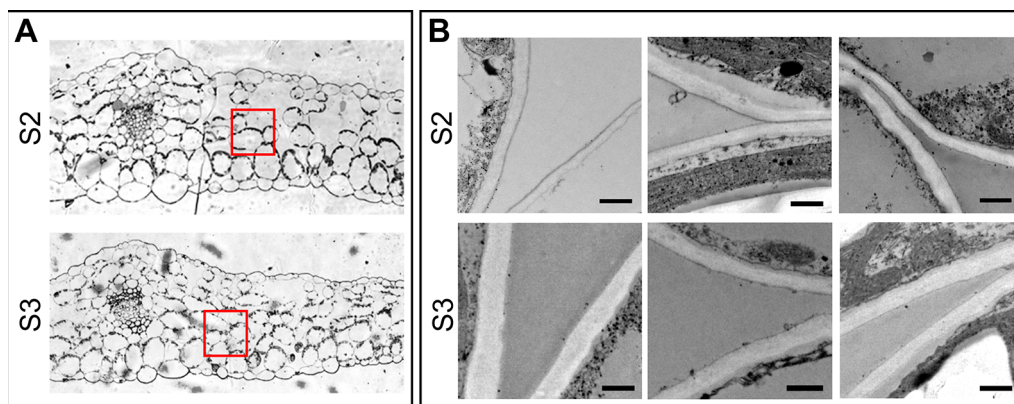


FIGURE 3 | Cell wall thickness of spongy mesophyll cells. (A) Transverse section of the middle part of the leaf, showing the areas examined for cell wall thickness. (B) Electron microscopy of the selected areas in panel A. Upper panel: S2 leaves, lower panel: S3 leaves. Scale bar 500 nm. Cell wall thickness was examined in different cells of at least three different leaves of each Stage. Measurements were taken at different points on the images, the number of total measurements for S2 and S3 were: *n* = 639 and *n* = 739, respectively. Obtained values were analyzed by one-way ANOVA, and Univariate Tests of Significance: *n* (S2 = 639, S3 = 739), mean ± SEM (S2 = 247.9 ± 3.0 nm, S3 = 278.8 ± 2.9), *F* = 63.02, *P* ≤ 0.0001.

these authors examined cell wall thickness in young and older leaves in the plant, whereas the present study compares non-senescent and senescent leaves that represent the same cohort at two different times of plant development.

Apoplastic Alkalinization Accompanies Developmental Leaf Senescence

Transient oscillations and long term changes in apoplastic pH (pH_{Apo}) trigger and/or modulate a myriad of signaling and metabolic pathways (Felle, 2001). Possible fluctuations in the pH_{Apo} between S2 and S3 leaves were evaluated by *in vivo* imaging using the genetically encoded pH sensor Apo-pHusion. Apo-pHusion plants stably express the mRFP1-EGFP tandem targeted to the apoplast (Gjetting et al., 2012). Confocal images

were acquired at the center of the leaf blade, from epidermal cells, where the fluorescence signal is strong enough to be quantified (Figure 4). The pH for each region of interest (ROI) was estimated based on the ratio between EGFP and mRFP1 fluorescence intensities, according to a calibration curve (Figures 4C, D). Estimated pH_{Apo} shifted around 0.8 units between S2 and S3, from $pH\ 5.43 \pm 0.03$ in S2 leaves to 6.26 ± 0.05 in S3 leaves (Figures 4A, B). These pH_{Apo} values are in the range of pH 5 to 6 expected for leaf pH_{Apo} (Felle, 2001), although absolute pH values may be difficult to estimate as they might be influenced by different factors, i.e. calibration. A pH_{Apo} shift of around 1 unit has been reported associated to electrical waves related to long distance signaling triggered by stress (Felle and Zimmermann, 2007). Different types of stress lead to a rise in pH_{Apo} and in extracellular ABA level, a promoter of leaf

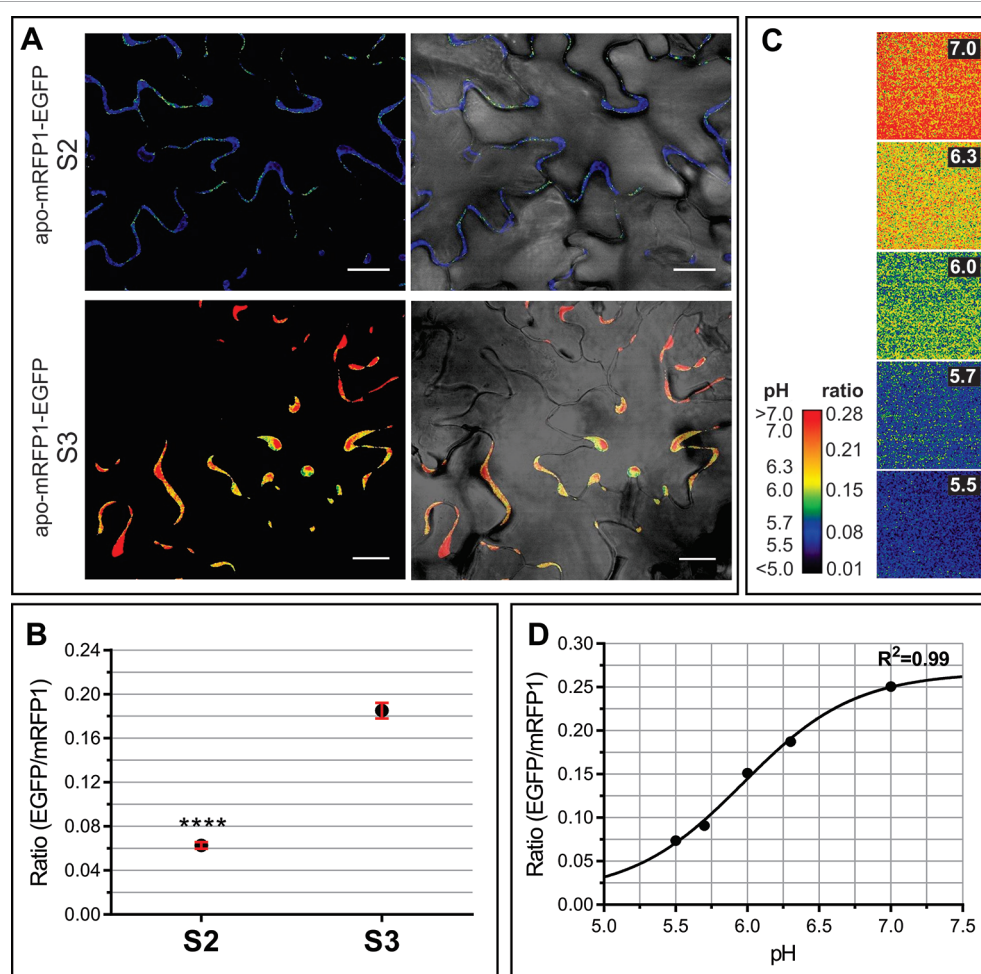


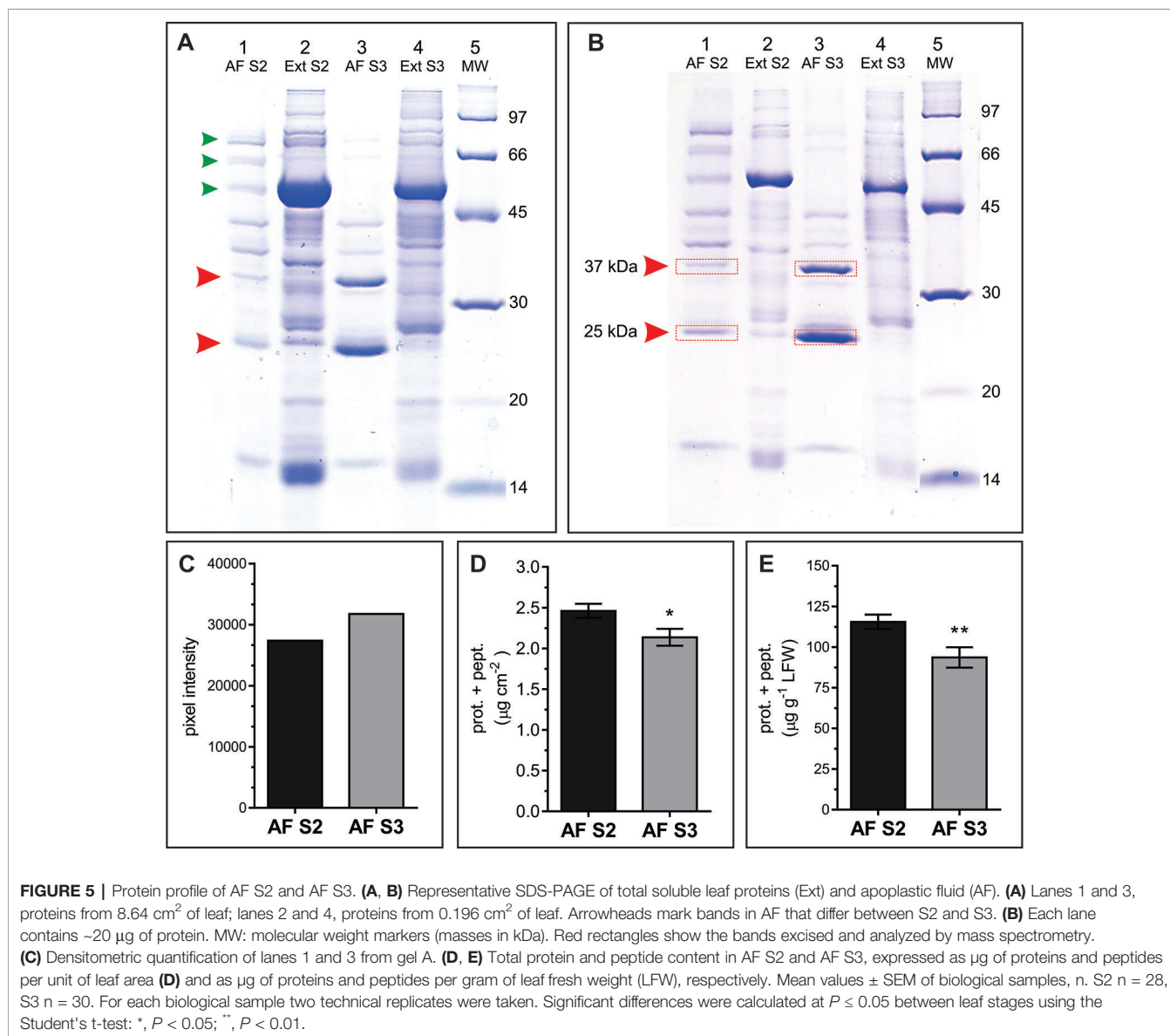
FIGURE 4 | Apoplastic pH of S2 and S3 leaves. *In vivo* analysis of apoplastic pH using the *Arabidopsis* transgenic line apo-mRFP1-EGFP (Gjetting et al., 2012). The pH was estimated according to the fluorescence intensity ratio EGFP/mRFP for each region of interest (ROI). **(A)** Left panels show representative ratio images of the leaf epidermis in S2 and S3 leaves, right panels show the merge of ratio images with their corresponding light field. **(B)** EGFP/mRFP ratio of leaf S2 and S3 epidermal cells. The values shown correspond to the mean \pm SEM of 39 and 119 ROIs from S2 and S3 leaves, respectively, taken from at least three different leaves for each stage. A Student t test ($P \leq 0.05$) was performed, asterisks indicate significant differences: ****, $P < 0.0001$. **(C, D)** *Ex vivo* calibration of the apo-pHusion sensor. **(C)** Ratio images of AWF incubated at different pH units, used to construct the calibration curve. For visual image presentation of ratio images, a pseudocolor look-up table was designed. **(D)** Calibration curve. PH was estimated according to the intensities of GFP and RFP fluorescence. Confocal data acquisition was performed on a Leica TCS SP5 II confocal laser scanning microscope. Image data were analyzed using the ImageJ software. Scale bar = 20 μm.

senescence (Zhao et al., 2016; Geilfus, 2017). It is controversial whether apoplast alkalization acts as an upstream signal triggering stress responses, or it is a consequence or secondary effect of the stress response (Geilfus, 2017), this controversy could be extended to the senescence-related scenario. Changes in Apo_{pH} affect the activity of extracellular enzymes and transporters, modulating different metabolic pathways (Hothorn et al., 2010).

The NH_3 released to the extracellular space during developmental and dark-induced senescence converts into NH_4^+ , that alkalizes the apoplast (Mattsson and Schjoerring, 2003). NH_4^+ accumulation and pH_{Apo} alkalization rates correlate with the progress of senescence in tobacco (Wu et al., 2016). A rise in pH_{Apo} leads to the ionization of wall molecules, i.e. pectin carboxyl groups, therefore more molecules of water are able to interact with these moieties, which could lead to an increase of cell wall thickness and V_{AF} .

Protein Profile of Apoplastic Fluids. Pathogenesis Related Proteins, PR, Accumulate in the Apoplast of Senescing Leaves

AWFs along with the corresponding whole leaf extracts from S2 and S3 leaves were examined in SDS-PAGE gels. In the range of 14 to 100 kDa, the AF protein patterns from S2 and S3 leaves (AFS2 and AFS3) displayed clear quantitative and qualitative differences (Figure 5). The AFS2 profile shows less protein per unit leaf area than the AFS3, and it is composed of several uniformly distributed protein bands. Few bands from 45 to 97 kDa are distinguished in AFS2 but not in AFS3 (Figure 5A, small arrowheads). The AFS3 protein profile is characterized by two conspicuous bands, one of apparent molecular mass of 25 kDa and another of 37 kDa, that are not clearly recognizable in AFS2 or in total leaf protein profiles (Figures 5A, B, big



arrowheads). The densitometric analysis of SDS-PAGE gels measured a higher protein content per unit leaf area in AFS3 than in AFS2 (**Figure 5C**) whereas, on the other hand, a colorimetric absorbance assay (Pierce™ BCA Protein Assay Kit), that detects all molecular weight proteins and peptides, reveals a higher protein and peptide content in AFS2 than in AFS3 either on a leaf area or LFW basis (**Figures 5D, E**). The discrepancy between methods might indicate a decline in the relative abundance of low molecular weight proteins (<14 kDa) and peptides in AFS3.

To identify the proteins corresponding to the two main bands detected in AFS3 protein profiles (**Figure 5A**) equal amounts of AFS2 and AFS3 proteins were loaded on an SDS-PAGE gel (**Figure 5B**), and the 25 and 37 kDa bands from S2 and S3 were cut off the gel and eluted for mass spectrometry analysis.

Peptide sequences identified different proteins in each band. According to the total number of peptide sequences for each identified protein (#PSM), the most abundant proteins were Pathogenesis-related protein 5 (PR5, At1g75040) in the 25 kDa band and endo-1,3 Glucan-beta-glucosidase, acidic isoform (PR2, At3g57260) in the 37 kDa band. Other less represented proteins co-migrating with PR2 and PR5 in the SDS-PAGE were also identified (**Supplemental Tables S1 and S2**). Both PR2 and PR5 contain an N-terminal signal peptide (SP) for secretion, and PR5 was previously detected in the N-glycosylated sub-proteome

of *Arabidopsis* mature stems (Wei et al., 2015). According to sequence homology, PR5 is a thaumatin-like protein (TLP) (Uknes et al., 1992). TLP have antifungal and antifreeze properties and accumulate in response to stress (Velazhahan et al., 1999). PR2 is a cell wall β -1,3-glucanase that hydrolyses the β -1,3 glucosidic bonds of β -1,3-glucans (callose) (Uknes et al., 1992). Besides being found in plant cells, β -1,3-glucans constitute the main structural components of fungal cell walls, hence the antifungal properties of PR2 (Doxey et al., 2007). PR5 and PR2 expression is associated with the hypersensitive response (HR), and systemic acquired resistance (SAR) (Geraats et al., 2007; Mishina and Zeier, 2007), and are widely considered hallmark genes for Salicylic acid (SA)-mediated defense and PCD (Uknes et al., 1992; Van Loon and Van Strien, 1999; Sävenstrand et al., 2004; Seo et al., 2008). However, PR2 and PR5, along with other PR genes are also induced in a SA partially independent manner, for instance, as part of signaling pathways mediated by the protein Di19 in *Arabidopsis* under drought-stress (Liu et al., 2013) and by the plasma membrane-localized, dark induced senescence associated Receptor-Like Kinase, OsSIK2, in rice (Chen et al., 2013).

PR2 and PR5 genes are up regulated during leaf senescence (Winter et al., 2007). PR5 expression is induced by the senescence-age related transcription factor WRKY75 in a SA mediated pathway (Guo et al., 2017). WRKY75 also represses

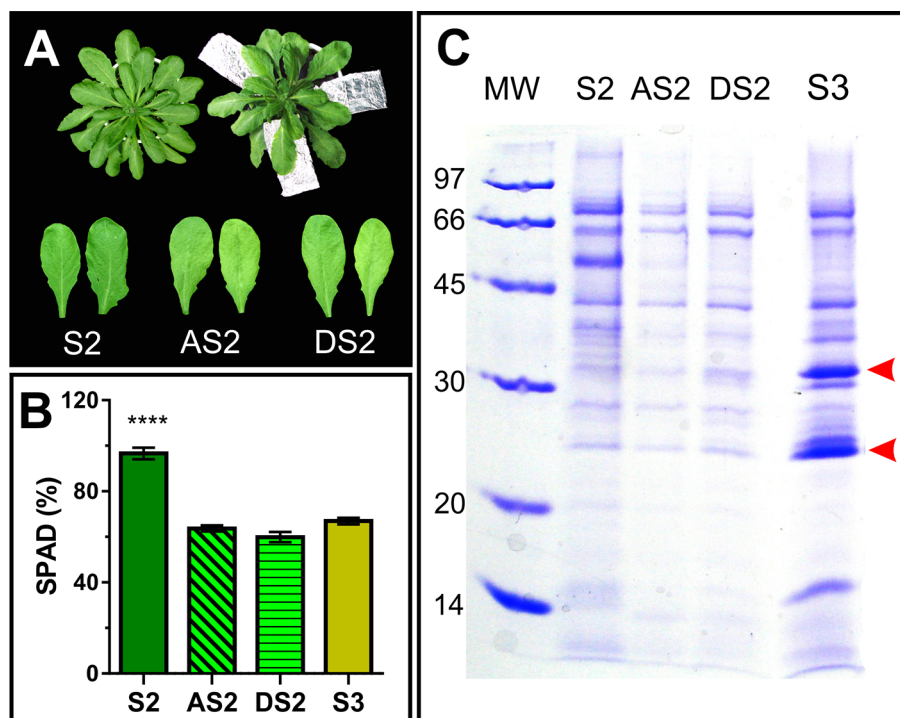


FIGURE 6 | Dark induced senescence of S2 leaves. **(A)** Attached S2 leaves (AS2) were wrapped in aluminum foil, and detached S2 leaves (DS2) were placed on moist filter paper in dark boxes, until their chlorophyll content reached S3 values (**Figure 1**). **(B)** Leaf chlorophyll content was measured non-destructively with the SPAD meter in different leaves, each of them represents a biological sample (n). S2: n = 29, AS2: n = 22, DS2: n = 5, S3: n = 18. For each biological sample, two SPAD readings were taken. Asterisks represent statistical differences between S2 vs. AS2, DS2 and S3 SPAD values (Dunnett's multiple comparisons test). **(C)** SDS-PAGE of AF from S2, dark induced attached and detached S2 (AS2 and DS2, respectively) and S3 leaves, compared per leaf area. Arrowheads show AF S3-associated bands.

catalase activity, a down regulator of *PR2* expression (Jing et al., 2009).

To dissect whether the accumulation pattern of *PR2* and *PR5* in the apoplast, is associated to the senescence syndrome or age-related, S2 leaves were induced to senesce in the dark for further AF evaluation. To this end, attached and detached S2 leaves where exposed to dark until their Chl content dropped down to S3 leaf values (Figures 6A, B). Dark-induced senescent S2 leaves attached and detached from the plant show lower AF protein content than that of control S2 leaves, and no accumulation of *PR2* and *PR5* (Figure 6C), suggesting that *PR2* and *PR5* proteins accumulate in the apoplast as part of developmental senescence, but not when senescence is imposed by dark incubation.

Apoplastic Fluid Proteome Dynamics During Developmental Leaf Senescence

For a more comprehensive repertoire of senescence related AF proteins, AWFs of S2 and S3 leaves were compared by shotgun proteomics. As a result, 212 proteins were identified, 183 of them showed a significant change (at least twofold difference between AFS2 and AFS3), and were considered AF senescence-related proteins, AFSP. Around 13% (24 proteins) of AFSP increased in the apoplast fluid of senescent leaves, S3 (Table 3), whereas 87% (159 proteins) of AFSP decreased during senescence (Supplemental Table S3).

Approximately half of the identified AFSP proteins lack of N-terminal signal peptide (SP), as described in extracellular proteomes before (Agrawal et al., 2010). All the 24 proteins that increased in AFS3 contain SP, whereas only 41.5% of the proteins that decreased in AFS3 contain SP (Figure 7A), suggesting that unconventional protein secretion mechanisms that locate leaderless secreted proteins to the apoplast might be less active during leaf senescence. N-glycosylations are posttranslational modifications required for proper folding, transport and/or function of secreted proteins (Song et al., 2013), and the extent and type of N-glycan structure varies as leaf ages (Elbers et al., 2001). Potential glycosylation sites are slightly more represented in proteins that increased in AFS3 compared to those that decline during senescence (Figure 7B).

AFSPs were classified into thirteen functional classes (Figure 7C), those proteins with several known functions were assigned to more than one functional group. AFS3 proteins relate to the main stress-response group, whereas AFS2 proteins relate mainly to two groups: stress-response and photosynthesis/carbohydrate metabolism.

Proteins That Accumulate in the Apoplast of Senescent Leaves

PR2 and *PR5* were identified among the proteins that accumulate in AFS3. Other 14 proteins significantly accumulate in AFS3 with respect to AFS2: peroxidases: *PRX34* (At3g49120), *PRX53* (At5g06720), and *PRX54* (At5g06730), lectin-like proteins, LLP, (At3g16530 and At3g15356), a cysteine protease (CP1A-5, At3g49340), a serine protease inhibitor (At2g43510), a phosphodiesterase

At4g36945, one amylase (*AMY1*, At4g25000), chitinases (At2g43580, At2g43570, and At3g54420), and ribonucleases (*PR4*, At3g04720, and *RNS1*, At2g02990). Eight proteins were specifically detected in AFS3 (not in AFS2): the peroxidases *PRX52* (At5g05340) and *PRX58* (At5g19880), one lipid transfer protein *LTP4* (At5g59310), a serine/threonine kinase (At1g51890), a nodulin-like protein (At5g53870), one glucanase (At4g16260), a germin-like protein (*GLP6*, At5g39100), and the metallo-protease (3-MMP, At1g24140). According to the information retrieved from the gene expression analysis platform EFP-Browser (Winter et al., 2007), all the identified AFS3 corresponding genes are up-regulated in senescing leaves, with the exception of chitinase At2g43580, whose expression remains unchanged.

Interestingly, all the AFS3 identified proteins have been related to stress responses, in particular to biotic stress, with the exception of *ENODL1* like protein At5g53870, that was shown to be promoted by drought and heat (Rizhsky et al., 2004); and only few AFS3 proteins have been previously related to leaf senescence. One of them is the amylase *AMY1*, that locates to the apoplast where it might degrade cell wall associated carbohydrates during *Arabidopsis* senescence (Doyle et al., 2007; Kamranfar et al., 2018), *AMY1* expression is also induced by ABA, heat, and pathogen-related stresses (Doyle et al., 2007). *Arabidopsis amy1* plants show early flowering (Jie et al., 2009). The ribonuclease *RNS1* has also been associated to senescence, with a potential role in Pi recycling (Bariola et al., 1994; Bariola et al., 1999). *RNS1* is markedly promoted by Pi deficit and *RNS1* protein accumulates in the secretome of Pi starved cells (Tran and Plaxton, 2008). *RNS1* expression is also associated to wounding induced local and systemic signaling (Lebrasseur et al., 2002), and correlates with the accumulation of specific tRNA fragments (Megel et al., 2019). The role of the other identified ribonuclease, *PR4*, is less known, its expression is associated with SAR (Mishina and Zeier, 2007), and its induced by ethylene and SA (Potter et al., 1993; Camargo-Ramírez et al., 2018).

The five AFS3 peroxidases have been related to pathogen responses. *PRX34* is sharply up regulated during senescence (Winter et al., 2007). *PRX34* was identified in the N-glycan secretome of *Arabidopsis* mature stems (Wei et al., 2015) and is also over accumulated under abiotic stress (Mano et al., 2014). *Arabidopsis* knock down plants for *PRX34* and its homolog *PRX33* (*prx34/prx33*) produce less apoplastic H₂O₂ as MAMPs (Microbe-associated molecular patterns) compared to wild type plants (Daudi et al., 2012) and are more sensitive to pathogen attack (O'Brien et al., 2012; Mammarella et al., 2015). *PRX34* along with *PRX52* accumulate in the leaf apoplast upon *Verticillium longisporum* infection (Floerl et al., 2012). The expression of *PRX54*, is also upregulated in response to fungal infection (Zhao et al., 2007), whereas *AtPRX53* is up regulated in response to nematodes, at their penetration sites, and also in response to wounding and jasmonic acid treatments (Jin et al., 2011). The lipid transfer protein *LTP4* accumulates in the AF, along with *PR5* and other PR genes, as part of the systemic resistance response induced by *Trichoderma* sp. and *P. syringae*

TABLE 3 | AF proteins with two fold increased levels during leaf senescence.

Protein	Protein ID	Gen ID	MW (kDa)	SL SUBA4	Biological process Gene Ontology	Biotic (B)/ (A) abiotic associated	gene expression during senescence	SP	N-g.s.	CL	Fold change
Probable LRR receptor-like protein kinase	C0LGG6	At1g51890	98.5	Ap, M, PM, N, ER, G	Protein phosphorylation, defense response to bacterium	B	↑	Yes	Yes	**	
PLC-like phosphodiesterases superfamily protein.	F4JQJ7	At4g36945	44.3	Ap, PM, ER, N, G, V	Lipid metabolism	B	No inf.	Yes	Yes	***	2.26
Endochitinase At2g43580	O24598	At2g43580	28.8	Ap, ER, G, V	Cell wall macromolecule catabolic process, response to fungus	B	—	Yes	Yes	***	4.75
Endochitinase (CHI, LSC222)	O24603	At2g43570	29.8	Ap, Mit, PM, ER, G, V	Cell wall macromolecule catabolic process, leaf senescence, response to virus, systemic acquired resistance	B	↑	Yes	Yes	****	4.12
Pathogenesis-related protein 5 (PR5)	P28493	At1g75040	25.2	Ap, V, Mit, ER, G, Cyt	Regulation of anthocyanin biosynthetic process, response to cadmium ion, response to UV-B, response to biotic stimuli, response to virus, systemic acquired resistance	B	↑	Yes	Yes	****	2.42
Glucan endo-1,3-beta-glucosidase, acidic isoform (PR2, BGL2)	P33157	At3g57260	37.3	Ap, PM, ER, V, G, Cyt, Chl	Carbohydrate metabolic process, response to cold, systemic acquired resistance, response to biotic stimuli	B-A	↑	Yes	Yes	****	4.06
Ribonuclease 1 (RNS1)	P42813	At2g02990	25.4	Ap, PM, ER, V, G	Aging, anthocyanin-containing compound biosynthetic process, cellular response to phosphate starvation, response to wounding	B-A	↑	Yes	Yes	****	6.44
Hevein-like preproprotein (HEL, PR4)	P43082	At3g04720	22.9	Ap, ER, G, V, Chl	Defense response to bacteria and fungi, killing of cells of other organism, response to ethylene, response to salicylic acid, response to herbivore, response to salt stress, response to virus, systemic acquired resistance	B	↑	Yes	No	***	2.83
Peroxidase 58 (PRX58)	P59120	At5g19880	35.4	Ap, Cyt, ER, G, PM, Chl	H ₂ O ₂ catabolic process, oxidation-reduction, response to ethylene, response to oxidative stress, response to pathogens	B	↑	Yes	Yes	**	
Germin-like protein subfamily 1 member 13 (GLP6)	P92997	At5g39100	24.1	Ap, Cyt, ER, G, Mit, N, Chl	Unknown	B	↑	Yes	Yes	**	
Peroxidase 53 (PRX53)	Q42578	At5g06720	35.0	Ap, G, Cyt, ER, N, Chl, V	H ₂ O ₂ catabolic process, oxidation-reduction, defense response to nematodes, response to oxidative stress, flower development	B	—	Yes	Yes	****	4.81
Metalloendoproteinase 3-MMP (At3-MMP)	Q5XF51	At1g24140	43.0	Ap, PM, M, G, ER, Mit, PX, Chl	Proteolysis, stress response	B-A	↑	Yes	Yes	**	
Alpha-amylase 1 (AMY1)	Q8VZ56	At4g25000	47.3	Ap, Cyt, ER, G, Chl	Carbohydrate metabolic process, response to ABA, response to gibberellins, stress response	B-A	↑	Yes	Yes	***	2.78
Probable glucan endo-1,3-beta-glucosidase	Q8VZJ2	At4g16260	37.7	Ap, T, PM, ER, G, Chl	Carbohydrate metabolic process, defense response to fungus, defense response to nematodes, response to salt stress	B-A	↑	Yes	No	***	
Peroxidase 54 (PRX54)	Q9FG34	At5g06730	37.3	Ap, T, V, ER, Cyt, G, N, PM, Chl	H ₂ O ₂ catabolic process, oxidation-reduction, response to oxidative stress	B-A	↑	Yes	Yes	***	5.06
Peroxidase 52 (PRX52)	Q9FLC0	At5g05340	34.2	Ap, Cyt, G, ER, N,	H ₂ O ₂ catabolic process, lignin biosynthetic process, oxidation-	B	↑	Yes	Yes	**	

(Continued)

TABLE 3 | Continued

Protein	Protein ID	Gen ID	MW (kDa)	SL SUBA4	Biological process Gene Ontology	Biotic (B)/ (A) abiotic associated	gene expression during senescence	SP	N-g.s.	CL	Fold change
Early nodulin-like protein 1 (ENODL1)	Q9FN39	At5g53870	38.4	Ap, PM, M, ER, G, N, V	reduction, response to oxidative stress, xylem development Electron transport chain, stress response	A Rizhsky et al. (2004)	↑	Yes	Yes	**	
Lectin-like protein LEC (LEC)	Q9LJR2	At3g15356	29.7	Ap, Mit, PM, Chl, G, ER, Cyt, N	Response to chitin, response to ethylene, response to jasmonic acid, defense response to fungus, ethylene-activated signaling pathway, response to wounding	B	No inf.	Yes	Yes	**	2.93
Lectin-like protein	Q9LK72	At3g16530	30.5	Ap, N, PM, ER, Cyt, G	Response to oomycetes, response to chitin	B	—	Yes	Yes	***	5.20
Non-specific lipid-transfer protein 4 (LTP4)	Q9LLR6	At5g59310	11.4	Ap, M, ER, G, Mit, Chl	Lipid transport, response to ABA, response to salt stress, water deprivation, pathogen	B-A	↑	Yes	No	**	
Cysteine protease-like protein	Q9SG15	At3g49340	37.7	Ap, ER, Cyt, G, Chl, V	Proteolysis	B Little et al. (2007)	↑	Yes	Yes	**	4.66
Peroxidase 34 (PRX34)	Q9SMU8	At3g49120	38.8	Ap, G, T, V, ER, Mit, N, PM, Chl	Defense response to bacterium, defense response to fungus, H2O2 catabolic process, oxidation-reduction, response to cytokinin, response to light stimuli, response to oxidative stress, unidimensional cell growth	B-A	↑	Yes	Yes	***	4.03
Defensin-like protein 195 (ATTI-1)	Q42328	At2g43510	9.9	Ap, G, Cyt, V, ER	Defense response, defense response to fungus, killing of cells of other organism	B	↑	Yes	No	***	2.36
Endochitinase EP3 (EP3)	Q9M2U5	At3g54420	29.4	Ap, G, Chl, V, ER	Cell wall macromolecule catabolic process, chitin catabolic process, defense response, hypersensitive response, polysaccharide catabolic process, response to bacterium, response to wounding, somatic embryogenesis	B-A	↑	Yes	Yes	**	2.00

Four samples (biological replicates) for each leaf stage were analyzed. A confidence level (CL) was assigned to each protein based on the number of biological replicates in which it appears: **, present in two biological replicates; ***, present in three biological replicates and ****, present in the four biological replicates. Rows highlighted in gray: proteins detected only in AF S3. Gene expression patterns associated with senescence (column "gene expression during senescence") were examined using the eFP Browser software (Winter et al., 2007). Subcellular locations and protein functions were determined using the SUBA4 (Hooper et al., 2016) and Gene Ontology (Ashburner et al., 2000; Consortium, 2016) databases. In bold, manually-assigned locations and in normal font, locations that were inferred from electronic annotation (IEA) or predicted. Biotic (B) or abiotic (A) stress related function were assigned according to Gene Ontology, or otherwise experimental data from literature. Presence of SP was determined by the SignalP 4.1 software (Petersen et al., 2011), and presence of potential N-glycosylation sites was determined with the ScanProsite tool (De Castro et al., 2006).

ID, identification; SL, subcellular localization; SP, signal peptide; N-g.s., potential N-glycosylation sites; CL, confidence level; M, membrane; PM, plasma membrane; G, Golgi; N, Nucleo; Cyt, cytoplasm; Chl, chloroplast; Mit, mitochondrion; Ap, apoplast; ER, endoplasmic reticulum; PX, peroxisome; V, vacuole; T, tonoplast; EV, extracellular vesicles (Rutter and Innes, 2017)

in *Arabidopsis* (Brotman et al., 2012). Two proteases with unknown function accumulate in the AF of S3 leaves. The metallo-protease 3-MMP belongs to the At-MMP family, predicted to be extracellular and related to pathogen responses (Zhao et al., 2017), though *at2-mmp* plants exhibited early senescence and late flowering (Gollack et al., 2002). The cysteine protease At3g49340 is up regulated in response to butterfly egg deposition, causing localized cell death at the site of oviposition (Little et al., 2007). Extracellular cysteine proteases have been shown to mediate defense responses by processing an apoplast immune signaling peptide (Ziemann et al., 2018). At3g49340 might play a similar role in senescence related signaling pathways.

The Germin like protein GLP6, is the only of the identified AFS3 proteins whose expression is down regulated under stress, either abiotic stress, like salt treatment (He et al., 2005), and biotic stress, for example at the galls formed in *Arabidopsis* roots upon infection with parasitic nematodes (Fuller et al., 2007).

Proteins That Decrease in the Apoplast of Senescent Leaves

The transcript levels of most of the identified proteins that decrease in AFS3 leaves remains unchanged or is down regulated during senescence, except for the aldolase *FBA6* (At2g36460), the acid phosphatase AtPAP26 (At5g34850), and the peroxidase *PRX51* (At4g37530), that remain constant or are

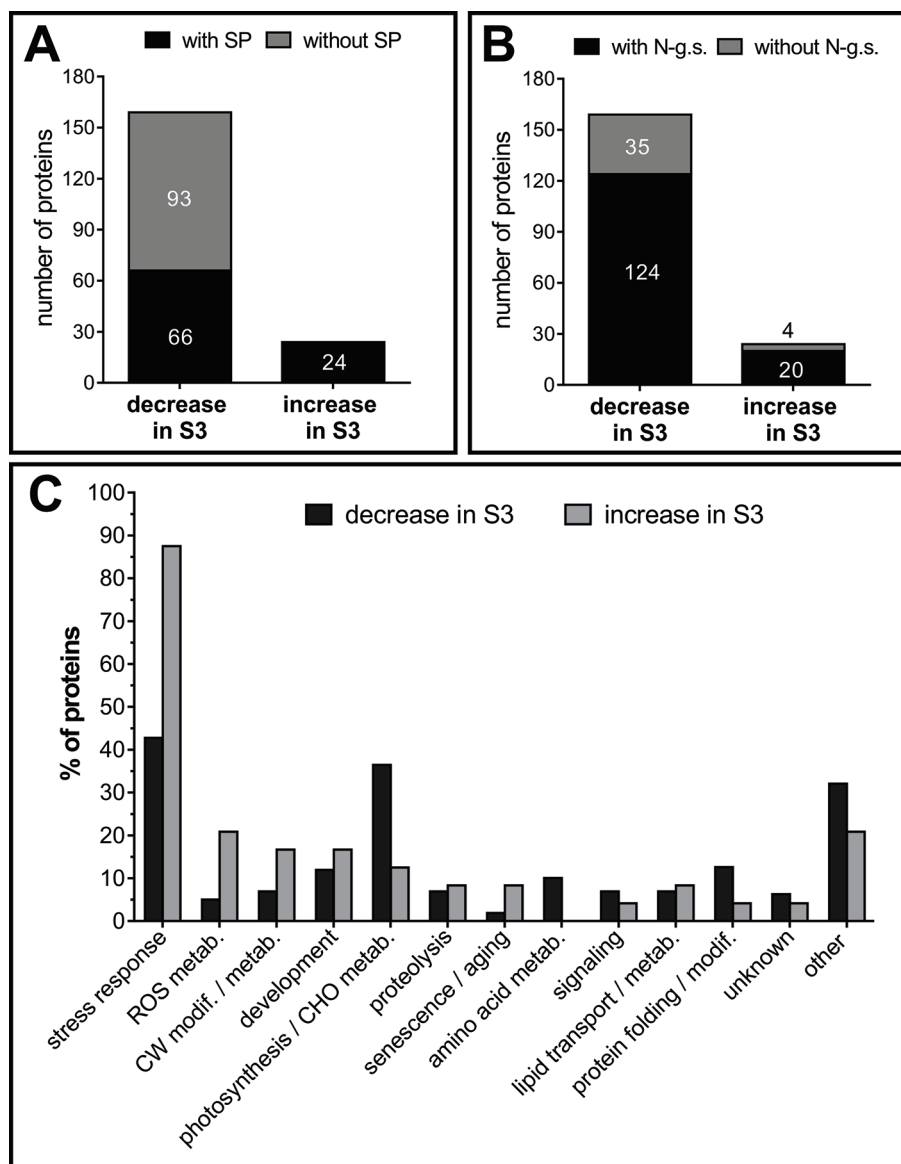


FIGURE 7 | Classification of AF proteins. Presence of signal peptide, SP, (A) and potential glycosylation sites (B). Numbers inside and outside the bars indicate the number of proteins. (C) Functional classification of AF proteins. Proteins with several known functions were assigned to more than one functional group. Values refer to the percentage of each functional sites group within the group of proteins that decrease in S3 and within the group of proteins that increase in S3. SP, signal peptide; N-g.s, potential N-glycosylation sites; CW, cell wall; ROS, reactive oxygen species; modif., modification; metab, metabolism; CHO, carbohydrate.

slightly up regulated during leaf senescence (Winter et al., 2007). Based on Gene Ontology (Ashburner et al., 2000) some of the AFSP that decrease in senescing leaves are also stress related, even though no prevalence of biotic stress over abiotic was observed as in ASF3 (Supplemental Table S3).

Among ASF2 proteins, the lipid transfer protein LTP6 (At1g55260) was shown to be involved in pathogen elicited responses, and its loss of function increases the susceptibility to penetration of the epidermal cell wall by powdery mildew (Fahlberg et al., 2019). Another LTP (At5g48490), identified only in AFS2, has also been related to SAR responses (Champigny et al., 2013).

The β -glucanase BG3 (At3g57240), the aspartic protease AED (At1g09750, Apoplastic, EDS1-Dependent), and the subtilase SBT 1.7 At5g67360 have also been described as part of pathogen responses, particularly associated to virus infection and to wounding (Golldack et al., 2003; Zavaliev et al., 2013; Breitenbach et al., 2014). The β galactosidase β G60 (At3g13750) was only detected in the AF of S2 leaves; its expression is up regulated by MBF1c (stress-response transcriptional coactivator multiprotein bridging factor) that enhances the tolerance to bacterial infection, heat, and osmotic stress (Suzuki et al., 2005).

Other abiotic stress inducible proteins specifically identified in AFS2 (absent in AFS3), are KIN2 (At5g15970), that responds

strongly to ABA, drought and salinity stresses (Kurkela and Borg-Franck, 1992; Zhang et al., 2018), and the pectin methyl esterase At2g46930, that is up regulated under cold stress (Provart et al., 2003).

Few of the identified AFS3 down regulated proteins have been linked to senescence, however, some of them might play specific roles related to senescence. For instance, the chaperone CPN-60 β 1 (At1g55490) was previously detected in the apoplast (Bindschedler et al., 2008), and the lack of its activity leads to growth rate reduction and cell death in *Arabidopsis* (Ishikawa et al., 2003) and tobacco (Zabaleta et al., 1994). Anxin AnnAt1 (At1g35720) was detected before in the apoplast (Clark et al., 2005; Bindschedler et al., 2008; Ge et al., 2011), and *at1g35720* plants show early senescence and hypersensitivity to osmotic stress (Lee et al., 2004). Ectopic expression of AnnBj1, the homolog of AnnAt1 in *Brassica juncea*, in tobacco and cotton leads to delayed senescence and increased H₂O₂ levels (Jami et al., 2008; Divya et al., 2010).

Some identified enzymes related to ROS (Reactive oxygen species) synthesis and catabolism decrease in AFS3. The superoxide dismutases CSD1 (At1g08830) and CSD2 (At2g28190) are plastidic, but have also been detected in the apoplast (Cheng et al., 2009; Nguyen-Kim et al., 2016). The glyoxylate oxidases GOX1 (At3g14420) and GOX2 (At3g14415) are involved in ROS production. These enzymes lack a SP, but were detected in the apoplast of *Arabidopsis* exposed to oxidative stress (Bindschedler et al., 2008). Double mutant plants *amiRgox1/2* display accelerated leaf senescence (Dellero et al., 2016). AtPAP26 expression is mildly up regulated during senescence (Winter et al., 2007), however its protein level decreases in AFS3. AtPAP26 localized to the apoplast and to the central vacuole is involved in vacuolar Pi recycling and extracellular Pi recruitment (Hurley et al., 2010; Tran et al., 2010). Mutant *atpap26* plants show severe reduction in P recycling, seeds with low P content, and delayed senescence (Robinson et al., 2012).

Interestingly, all of the enzymes related to amino acid metabolism identified in this study decrease in AFS3 (**Supplemental Table S3**). Among them glutamate synthase Fd-GOGAT1 (GLU1, At5g04140) and glutamine synthetase 2 (At5g35630) localize to chloroplast and mitochondria but also to the apoplast (Taira et al., 2004; Bindschedler et al., 2008). Glycine decarboxylase GDCH (At2g35370) also localizes to chloroplast and mitochondria (Kleffmann et al., 2004; Huang et al., 2015), but has not been reported in the apoplast before. GDCH deficiency causes premature senescence in rice (Zhou et al., 2013). The cysteine synthase OASA1 (At4g14880) was previously detected in extracellular vesicles in *Arabidopsis* exposed to oxidative stress (Bindschedler et al., 2008; Rutter and Innes, 2017), and *at4g14880* plants show accelerated leaf senescence (Jing et al., 2002).

The Cyclophilin CYP20-3 (At3g62030) participates in protein folding and cysteine synthesis during stress (Lippuner et al., 1994; Dominguez-Solis et al., 2008; Park et al., 2013), and *cyp20-3* plants senesce faster under oxidative stress (Dominguez-Solis et al., 2008). CYP20-3 is chloroplast located (Lippuner et al., 1994; Hooper et al., 2016), though it was found in the apoplast (Bindschedler et al., 2008), and it would be secreted according to Plant-mPLOC software *in silico* simulations (Chou and Shen, 2010).

CONCLUSIONS

The two most abundant proteins in the apoplast of senescing leaves, PR2 and PR5, along with all the identified apoplastic proteins that increase during senescence, have been previously linked to stress responses.

Leaf senescence-related changes in the secretome, along with variations in the AF volume and pH resemble pathogen attack responses, that in turn involve the induction of many Senescence Associated Genes, SAGs genes (Little et al., 2007; Schippers et al., 2015). PR5 markedly accumulates in the apoplast in response to a variety of biotic and abiotic stresses (Piofczyk et al., 2015; Lambertucci et al., 2019), suggesting a role in a possible universal stress response, or in a crosstalk point where different stress responses converge. It would be plausible that stress-related and senescence programs trigger common mechanisms under conditions requiring recycling. Biotic and abiotic responses are differentially prioritized in a leaf dependent manner in *Arabidopsis* (Berens et al., 2019). Leaves of different ages differentially control responses to stress, allowing for a balance to maintain growth or survival at the organism level (Farber and Mundt, 2017; Berens et al., 2019).

Dark induced-senescence genes are up regulated in *Arabidopsis* infected with tobacco rattle virus, TRV (Fernandez-Calvino et al., 2016), however PR2 and PR5 showed no accumulation in the apoplast of mature healthy leaves (S2) induced to senesce in darkness (**Figure 6**). The specific accumulation of PR2 and PR5 in the apoplast during natural senescence, but not during dark induced senescence suggests that age-related signals, independently of the sink-source status of the leaf, might be priming the apoplast for stress responses in an as yet undamaged leaf. Salicylic Acid, SA, accumulates in an age-related way, and under SA basal levels defense responses are promoted and PR proteins accumulate.

Comparative proteomics of vascular sap reveals a common theme among apoplast fluid, xylem, and phloem sap proteomes collected from stressed plants, that is the accumulation of PR proteins including thaumatin-like proteins, chitinases, and glucanases (Rodríguez-Celma et al., 2016).

The extracellular space might thus represent an up-to-date dismissed scenario where developmental senescence and stress related pathways overlap and integrate.

DATA AVAILABILITY STATEMENT

This article contains previously unpublished data. The name of the repository and accession number(s) are available at https://figshare.com/projects/FPS_manuscript_476421_Senescence_related_changes_in_leaf_apoplast/71789.

AUTHOR CONTRIBUTIONS

MB, JG, and DM designed the experiments. MB and MM performed the experiments. DM and JG wrote the article. MB,

JG, and DM discussed the data and revised the article. All authors approved the final manuscript.

FUNDING

This work was supported by grant from Agencia nacional de Promoción Científica y Tecnológica, Pres. BID. Pict 1092.

ACKNOWLEDGMENTS

ApoPhusion line was kindly provided by Dr Fuglsang (Department of Plant Biology and Biotechnology, Faculty of

REFERENCES

- Agrawal, G. K., Jwa, N. S., Lebrun, M. H., Job, D., and Rakwal, R. (2010). Plant secretome: unlocking secrets of the secreted proteins. *Proteomics* 10, 799–827. doi: 10.1002/pmic.200900514
- Andersen, M., Jensen, C., and Losch, R. (1991). Derivation of pressure-volume curves by a non-linear regression procedure and determination of apoplastic water. *J. Exp. Bot.* 42, 159–165. doi: 10.1093/jxb/42.2.159
- Ashburner, M., Ball, C. A., Blake, J. A., Botstein, D., Butler, H., Cherry, J. M., et al. (2000). Gene ontology: tool for the unification of biology. *Nat. Genet.* 25, 25–29. doi: 10.1038/75556
- Bariola, P. A., Howard, C. J., Taylor, C. B., Verburg, M. T., Jaglan, V. D., and Green, P. J. (1994). The Arabidopsis ribonuclease gene RNS1 is tightly controlled in response to phosphate limitation. *Plant J.* 6, 673–685. doi: 10.1046/j.1365-3113.1994.6050673.x
- Bariola, P. A., Macintosh, G. C., and Green, P. J. (1999). Regulation of S-like ribonuclease levels in Arabidopsis. Antisense inhibition of RNS1 or RNS2 elevates anthocyanin accumulation. *Plant Physiol.* 119, 331–342. doi: 10.1104/pp.119.1.331
- Berens, M. L., Wolinska, K. W., Spaepen, S., Ziegler, J., Nobori, T., Nair, A., et al. (2019). Balancing trade-offs between biotic and abiotic stress responses through leaf age-dependent variation in stress hormone cross-talk. *Proc. Natl. Acad. Sci.* 116, 2364–2373. doi: 10.1073/pnas.1817233116
- Bindschedler, L. V., Palmblad, M., and Cramer, R. (2008). Hydroponic isotope labelling of entire plants (HILEP) for quantitative plant proteomics; an oxidative stress case study. *Phytochemistry* 69, 1962–1972. doi: 10.1016/j.phytochem.2008.04.007
- Blumenkrantz, N., and Asboe-Hansen, G. (1973). New method for quantitative determination of uronic acids. *Anal. Biochem.* 54, 484–489. doi: 10.1016/0003-2697(73)90377-1
- Boudart, G., Jamet, E., Rossignol, M., Lafitte, C., Borderies, G., Jauneau, A., et al. (2005). Cell wall proteins in apoplastic fluids of Arabidopsis thaliana rosettes: identification by mass spectrometry and bioinformatics. *Proteomics* 5, 212–221. doi: 10.1002/pmic.200400882
- Boyer, J. (1967). Matric potentials of leaves. *Plant Physiol.* 42, 213–217. doi: 10.1104/pp.42.2.213
- Breeze, E., Harrison, E., Mchattie, S., Hughes, L., Hickman, R., Hill, C., et al. (2011). High-resolution temporal profiling of transcripts during Arabidopsis leaf senescence reveals a distinct chronology of processes and regulation. *Plant Cell* 23, 873–894. doi: 10.1105/tpc.111.083345
- Breitenbach, H. H., Wenig, M., Wittek, F., Jorda, L., Maldonado-Alconada, A. M., Sarioglu, H., et al. (2014). Contrasting Roles of the Apoplastic Aspartyl Protease APOPLASTIC, ENHANCED DISEASE SUSCEPTIBILITY-DEPENDENT1 and LEGUME LECTIN-LIKE PROTEIN1 in Arabidopsis Systemic Acquired Resistance. *Plant Physiol.* 165, 791–809. doi: 10.1104/pp.114.239665
- Brotman, Y., Lisec, J., Meret, M., Chet, I., Willmitzer, L., and Viterbo, A. (2012). Transcript and metabolite analysis of the Trichoderma-induced systemic resistance response to Pseudomonas syringae in Arabidopsis thaliana. *Microbiology* 158, 139–146. doi: 10.1099/mic.0.052621-0
- Life Sciences, University of Copenhagen). The Dew point Psychrometer C-52 (Wescor®) and the Vapor pressure micro Osmometer belong to the Instituto de Investigaciones Fisiológicas y Ecológicas vinculadas a la Agricultura (IFEVA) and Instituto Leloir, respectively. The Vacuum Freeze Dryer belongs to Centro de Investigación de Proteínas Vegetales (CIProVe).
- Camargo-Ramírez, R., Val-Torregrosa, B., and San Segundo, B. (2018). MiR858-Mediated regulation of flavonoid-specific MYB transcription factor genes controls resistance to pathogen infection in Arabidopsis. *Plant Cell Physiol.* 59, 190–204. doi: 10.1093/pcp/pcx175
- Carpita, N. C., and Kanabus, J. (1987). Extraction of starch by dimethyl sulfoxide and quantitation by enzymatic assay. *Anal. Biochem.* 161, 132–139. doi: 10.1016/0003-2697(87)90662-2
- Chakraborty, S., Nascimento, R., Zaini, P. A., Gouran, H., Rao, B. J., Goulart, L. R., et al. (2016). Sequence/structural analysis of xylem proteome emphasizes pathogenesis-related proteins, chitinases and beta-1, 3-glucanases as key players in grapevine defense against Xylella fastidiosa. *PeerJ* 4, e2007. doi: 10.7717/peerj2007
- Champigny, M. J., Isaacs, M., Carella, P., Faubert, J., Fobert, P. R., and Cameron, R. K. (2013). Long distance movement of DIR1 and investigation of the role of DIR1-like during systemic acquired resistance in Arabidopsis. *Front. Plant Sci.* 4, 230. doi: 10.3389/fpls.2013.00230
- Chen, L. J., Wuriyangan, H., Zhang, Y. Q., Duan, K. X., Chen, H. W., Li, Q. T., et al. (2013). An S-domain receptor-like kinase, OsSIK2, confers abiotic stress tolerance and delays dark-induced leaf senescence in rice. *Plant Physiol.* 163, 1752–1765. doi: 10.1104/pp.113.224881
- Cheng, F. Y., Blackburn, K., Lin, Y. M., Goshe, M. B., and Williamson, J. D. (2009). Absolute protein quantification by LC/MS(E) for global analysis of salicylic acid-induced plant protein secretion responses. *J. Proteome Res.* 8, 82–93. doi: 10.1021/pr800649s
- Chou, K.-C., and Shen, H.-B. (2010). Plant-mPLoc: a top-down strategy to augment the power for predicting plant protein subcellular localization. *PLoS One* 5, e11335. doi: 10.1371/journal.pone.0011335
- Clark, G. B., Lee, D., Dauwalder, M., and Roux, S. J. (2005). Immunolocalization and histochemical evidence for the association of two different Arabidopsis annexins with secretion during early seedling growth and development. *Planta* 220, 621–631. doi: 10.1007/s00425-004-1374-7
- Coffeen, W. C., and Wolpert, T. J. (2004). Purification and characterization of serine proteases that exhibit caspase-like activity and are associated with programmed cell death in Avena sativa. *Plant Cell* 16, 857–873. doi: 10.1105/tpc.017947
- Consortium, G. O. (2016). Expansion of the Gene Ontology knowledgebase and resources. *Nucleic Acids Res.* 45, D331–D338. doi: 10.1093/nar/gkw1108
- Dani, V., Simon, W. J., Duranti, M., and Croy, R. R. (2005). Changes in the tobacco leaf apoplast proteome in response to salt stress. *Proteomics* 5, 737–745. doi: 10.1002/pmic.200401119
- Daudi, A., Cheng, Z., O'Brien, J. A., Mammarella, N., Khan, S., Ausubel, F. M., et al. (2012). The apoplastic oxidative burst peroxidase in Arabidopsis is a major component of pattern-triggered immunity. *Plant Cell* 24, 275–287. doi: 10.1105/tpc.111.093039
- De Castro, E., Sigrist, C. J., Gattiker, A., Bulliard, V., Langendijk-Genevaux, P. S., Gasteiger, E., et al. (2006). ScanProsite: detection of PROSITE signature matches and ProRule-associated functional and structural residues in proteins. *Nucleic Acids Res.* 34, W362–W365. doi: 10.1093/nar/gkl124

SUPPLEMENTARY MATERIAL

The Supplementary Material for this article can be found online at: <https://www.frontiersin.org/articles/10.3389/fpls.2019.01635/full#supplementary-material>

- Dellero, Y., Jossier, M., Glab, N., Oury, C., Tcherkez, G., and Hodges, M. (2016). Decreased glycolate oxidase activity leads to altered carbon allocation and leaf senescence after a transfer from high CO₂ to ambient air in *Arabidopsis thaliana*. *J. Exp. Bot.* 67, 3149–3163. doi: 10.1093/jxb/erw054
- Delorme, V. G., McCabe, P. F., Kim, D.-J., and Leaver, C. J. (2000). A matrix metalloproteinase gene is expressed at the boundary of senescence and programmed cell death in cucumber. *Plant Physiol.* 123, 917–928. doi: 10.1104/pp.123.3.917
- Dietz, K. J. (1997). “Functions and responses of the leaf apoplast under stress,” in *Progress in Botany*. Eds. H. D. Behnke, U. Lüttge, K. Esser, J. W. Kadereit and M. Runge (Berlin, Heidelberg: Springer), 221–254. doi: 10.1007/978-3-642-60458-4_9
- Divya, K., Jami, S., and Kirti, P. (2010). Constitutive expression of mustard annexin, AnnBj1 enhances abiotic stress tolerance and fiber quality in cotton under stress. *Plant Mol. Biol.* 73, 293–308. doi: 10.1007/s11103-010-9615-6
- Dominguez-Solis, J. R., He, Z., Lima, A., Ting, J., Buchanan, B. B., and Luan, S. (2008). A cyclophilin links redox and light signals to cysteine biosynthesis and stress responses in chloroplasts. *Proc. Natl. Acad. Sci.* 105, 16386–16391. doi: 10.1073/pnas.0808204105
- Doxey, A. C., Yaish, M. W., Moffatt, B. A., Griffith, M., and McConkey, B. J. (2007). Functional divergence in the *Arabidopsis* β -1, 3-glucanase gene family inferred by phylogenetic reconstruction of expression state. *Mol. Biol. Evol.* 24, 1045–1055. doi: 10.1093/molbev/msm024
- Doyle, E. A., Lane, A. M., Sides, J. M., Mudgett, M. B., and Monroe, J. D. (2007). An α -amylase (At4g25000) in *Arabidopsis* leaves is secreted and induced by biotic and abiotic stress. *Plant Cell Environ.* 30, 388–398. doi: 10.1111/j.1365-3040.2006.01624.x
- Elbers, I. J., Stoopen, G. M., Bakker, H., Stevens, L. H., Bardor, M., Molthoff, J. W., et al. (2001). Influence of Growth Conditions and Developmental Stage on N-Glycan Heterogeneity of Transgenic Immunoglobulin G and Endogenous Proteins in Tobacco Leaves. *Plant Physiol.* 126, 1314–1322. doi: 10.1104/pp.126.3.1314
- Fahlberg, P., Buhot, N., Johansson, O. N., and Andersson, M. X. (2019). Involvement of lipid transfer proteins in resistance against a non-host powdery mildew in *Arabidopsis thaliana*. *Mol. Plant Pathol.* 20, 69–77. doi: 10.1111/mpp.12740
- Farber, D., and Mundt, C. (2017). Effect of plant age and leaf position on susceptibility to wheat stripe rust. *Phytopathology* 107, 412–417. doi: 10.1094/PHYTO-07-16-0284-R
- Felle, H. H., and Zimmermann, M. R. (2007). Systemic signalling in barley through action potentials. *Planta* 226, 203. doi: 10.1007/s00425-006-0458-y
- Felle, H. H., Herrmann, A., Hanstein, S., Hüchelhoven, R., and Kogel, K.-H. (2004). Apoplastic pH signaling in barley leaves attacked by the powdery mildew fungus *Blumeria graminis* f. sp. *hordei*. *Mol. Plant-Microbe Interact.* 17, 118–123. doi: 10.1094/MPMI.2004.17.1.118
- Felle, H. (2001). pH: signal and messenger in plant cells. *Plant Biol.* 3, 577–591. doi: 10.1055/s-2001-19372
- Fernandez-Calvino, L., Guzman-Benito, I., Del Toro, F. J., Donaire, L., Castro-Sanz, A. B., Ruiz-Ferrer, V., et al. (2016). Activation of senescence-associated Dark-inducible (DIN) genes during infection contributes to enhanced susceptibility to plant viruses. *Mol. Plant Pathol.* 17, 3–15. doi: 10.1111/mpp.12257
- Floerl, S., Majcherczyk, A., Possienke, M., Feussner, K., Tappe, H., Gatz, C., et al. (2012). *Verticillium longisporum* infection affects the leaf apoplastic proteome, metabolome, and cell wall properties in *Arabidopsis thaliana*. *PLoS One* 7, e31435. doi: 10.1371/journal.pone.0031435
- Forouzesh, E., Goel, A., Mackenzie, S. A., and Turner, J. A. (2013). In vivo extraction of *Arabidopsis* cell turgor pressure using nanoindentation in conjunction with finite element modeling. *Plant J.* 73, 509–520. doi: 10.1111/tpj.12042
- Fuller, V. L., Lilley, C. J., Atkinson, H. J., and Urwin, P. E. (2007). Differential gene expression in *Arabidopsis* following infection by plant-parasitic nematodes *Meloidogyne incognita* and *Heterodera schachtii*. *Mol. Plant Pathol.* 8, 595–609. doi: 10.1111/j.1364-3703.2007.00416.x
- Ge, W., Song, Y., Zhang, C., Zhang, Y., Burlingame, A. L., and Guo, Y. (2011). Proteomic analyses of apoplastic proteins from germinating *Arabidopsis thaliana* pollen. *Biochim. Biophys. Acta* 1814, 1964–1973. doi: 10.1016/j.bbapap.2011.07.013
- Geilfus, C. M., Mithöfer, A., Ludwig-Müller, J., Zörb, C., and Muehling, K. H. (2015). Chloride-inducible transient apoplastic alkalinizations induce stomata closure by controlling abscisic acid distribution between leaf apoplast and guard cells in salt-stressed *Vicia faba*. *New Phytol.* 208, 803–816. doi: 10.1111/nph.13507
- Geilfus, C.-M. (2017). The pH of the apoplast: dynamic factor with functional impact under stress. *Mol. Plant* 10, 1371–1386. doi: 10.1016/j.molp.2017.09.018
- Geraats, B. P., Bakker, P. A., Linthorst, H. J., Hoekstra, J., and Van Loon, L. C. (2007). The enhanced disease susceptibility phenotype of ethylene-insensitive tobacco cannot be counteracted by inducing resistance or application of bacterial antagonists. *Physiol. Mol. Plant Pathol.* 70, 10. doi: 10.1016/j.mpp.2007.07.003
- Gjetting, S. K., Ytting, C. K., Schulz, A., and Fuglsang, A. T. (2012). Live imaging of intra- and extracellular pH in plants using pHusion, a novel genetically encoded biosensor. *J. Exp. Bot.* 63, 3207–3218. doi: 10.1093/jxb/ers040
- Gollmack, D., Popova, O. V., and Dietz, K.-J. (2002). Mutation of the matrix metalloproteinase At2-MMP inhibits growth and causes late flowering and early senescence in *Arabidopsis*. *J. Biol. Chem.* 277, 5541–5547. doi: 10.1074/jbc.M106197200
- Gollmack, D., Vera, P., and Dietz, K. J. (2003). Expression of subtilisin-like serine proteases in *Arabidopsis thaliana* is cell-specific and responds to jasmonic acid and heavy metals with developmental differences. *Physiol. Plant* 118, 64–73. doi: 10.1034/j.1399-3054.2003.00087.x
- Goulet, C., Goulet, C., Goulet, M. C., and Michaud, D. (2010). 2-DE proteome maps for the leaf apoplast of *Nicotiana benthamiana*. *Proteomics* 10, 2536–2544. doi: 10.1002/pmic.200900382
- Grudkowska, M., and Zagdanska, B. (2004). Multifunctional role of plant cysteine proteinases. *Acta Biochim. Pol.* 51, 609–624. doi: 10.18388/abp.2004_3547
- Guamet, J. J., Tyystjarvi, E., Tyystjarvi, T., John, I., Kairavuo, M., Pichersky, E., et al. (2002). Photoinhibition and loss of photosystem II reaction centre proteins during senescence of soybean leaves. Enhancement of photoinhibition by the ‘stay-green’ mutation cytG. *Physiol. Plant* 115, 468–478. doi: 10.1034/j.1399-3054.2002.1150317.x
- Guo, P., Li, Z., Huang, P., Li, B., Fang, S., Chu, J., et al. (2017). A tripartite amplification loop involving the transcription factor WRKY75, salicylic acid, and reactive oxygen species accelerates leaf senescence. *Plant Cell* 29, 2854–2870. doi: 10.1105/tpc.17.00438
- Gupta, R., Lee, S. E., Agrawal, G. K., Rakwal, R., Park, S., Wang, Y., et al. (2015). Understanding the plant-pathogen interactions in the context of proteomics-generated apoplastic proteins inventory. *Front. In Plant Sci.* 6, 352. doi: 10.3389/fpls.2015.00352
- Hamouda, I., Badri, M., Mejri, M., Cruz, C., Siddique, K., and Hessini, K. (2016). Salt tolerance of *Beta macrocarpa* is associated with efficient osmotic adjustment and increased apoplastic water content. *Plant Biol.* 18, 369–375. doi: 10.1111/plb.12419
- He, X. J., Mu, R. L., Cao, W. H., Zhang, Z. G., Zhang, J. S., and Chen, S. Y. (2005). AtNAC2, a transcription factor downstream of ethylene and auxin signaling pathways, is involved in salt stress response and lateral root development. *Plant J.* 44, 903–916. doi: 10.1111/j.1365-313X.2005.02575.x
- Higgins, R., Lockwood, T., Holley, S., Yalamanchili, R., and Stratmann, J. W. (2007). Changes in extracellular pH are neither required nor sufficient for activation of mitogen-activated protein kinases (MAPKs) in response to systemin and fusicoccin in tomato. *Planta* 225, 1535–1546. doi: 10.1007/s00425-006-0440-8
- Hooper, C. M., Castleden, I. R., Tanz, S. K., Aryamanesh, N., and Millar, A. H. (2016). SUBA4: the interactive data analysis centre for *Arabidopsis* subcellular protein locations. *Nucleic Acids Res.* 45, D1064–D1074. doi: 10.1093/nar/gkw1041
- Hoson, T. (1998). Apoplast as the site of response to environmental signals. *J. Plant Res.* 111, 167–177. doi: 10.1007/BF02507163
- Hothorn, M., Van Den Ende, W., Lammens, W., Rybin, V., and Scheffzek, K. (2010). Structural insights into the pH-controlled targeting of plant cell-wall invertase by a specific inhibitor protein. *Proc. Natl. Acad. Sci.* 107, 17427–17432. doi: 10.1073/pnas.1004481107
- Huang, S., Nelson, C. J., Li, L., Taylor, N. L., Ströher, E., Petereit, J., et al. (2015). INTERMEDIATE CLEAVAGE PEPTIDASE55 modifies enzyme amino termini and alters protein stability in *Arabidopsis* mitochondria. *Plant Physiol.* 168, 415–427. doi: 10.1104/pp.15.00300

- Hurley, B. A., Tran, H. T., Marty, N. J., Park, J., Snedden, W. A., Mullen, R. T., et al. (2010). The dual-targeted purple acid phosphatase isozyme AtPAP26 is essential for efficient acclimation of Arabidopsis to nutritional phosphate deprivation. *Plant Physiol.* 153, 1112–1122. doi: 10.1104/pp.110.153270
- Husted, S., and Schjoerring, J. K. (1995). Apoplastic pH and Ammonium Concentration in Leaves of *Brassica napus* L. *Plant Physiol.* 109, 1453–1460. doi: 10.1104/pp.109.41453
- Ishikawa, A., Tanaka, H., Nakai, M., and Asahi, T. (2003). Deletion of a chaperonin 60 β gene leads to cell death in the Arabidopsis lesion initiation 1 mutant. *Plant Cell Physiol.* 44, 255–261. doi: 10.1093/pcp/pcg031
- Jami, S. K., Clark, G. B., Turlapati, S. A., Handley, C., Roux, S. J., and Kirti, P. B. (2008). Ectopic expression of an annexin from *Brassica juncea* confers tolerance to abiotic and biotic stress treatments in transgenic tobacco. *Plant Physiol. Biochem.* 46, 1019–1030. doi: 10.1016/j.plaphy.2008.07.006
- Jie, W., Dashi, Y., Xinhong, G., and Xuanming, L. (2009). Arabidopsis AMY1 expressions and early flowering mutant phenotype. *BMB Rep.* 42, 101–105. doi: 10.5483/BMBRep.2009.42.2.101
- Jin, Y., Ni, D.-A., and Ruan, Y.-L. (2009). Posttranslational elevation of cell wall invertase activity by silencing its inhibitor in tomato delays leaf senescence and increases seed weight and fruit hexose level. *Plant Cell* 21, 2072–2089. doi: 10.1105/tpc.108.063719
- Jin, J., Hewezi, T., and Baum, T. J. (2011). Arabidopsis peroxidase AtPRX53 influences cell elongation and susceptibility to *Heterodera schachtii*. *Plant Signal Behav.* 6, 1778–1786. doi: 10.4161/psb.6.11.17684
- Jing, H. C., Sturte, M. J., Hille, J., and Dijkwel, P. P. (2002). Arabidopsis onset of leaf death mutants identify a regulatory pathway controlling leaf senescence. *Plant J.* 32, 51–63. doi: 10.1046/j.1365-313X.2002.01400.x
- Jing, S., Zhou, X., Song, Y., and Yu, D. (2009). Heterologous expression of OsWRKY23 gene enhances pathogen defense and dark-induced leaf senescence in Arabidopsis. *Plant Growth Regul.* 58, 9. doi: 10.1007/s10725-009-9366-z
- Kamranfar, I., Xue, G. P., Tohge, T., Sedaghatmehr, M., Fernie, A. R., Balazadeh, S., et al. (2018). Transcription factor RD26 is a key regulator of metabolic reprogramming during dark-induced senescence. *New Phytol.* 218, 1543–1557. doi: 10.1111/nph.15127
- Karpinska, B., Zhang, K., Rasool, B., Pastok, D., Morris, J., Verrall, S. R., et al. (2018). The redox state of the apoplast influences the acclimation of photosynthesis and leaf metabolism to changing irradiance. *Plant Cell Environ.* 41, 1083–1097. doi: 10.1111/pce.12960
- Kleffmann, T., Russenberger, D., Von Zychlinski, A., Christopher, W., Sjölander, K., Gruissem, W., et al. (2004). The *Arabidopsis thaliana* chloroplast proteome reveals pathway abundance and novel protein functions. *Curr. Biol.* 14, 354–362. doi: 10.1016/j.cub.2004.02.039
- Kosová, K., Vítámvás, P., Prášil, I. T., and Renaut, J. (2011). Plant proteome changes under abiotic stress—contribution of proteomics studies to understanding plant stress response. *J. Proteomics* 74, 1301–1322. doi: 10.1016/j.jpro.2011.02.006
- Kurkela, S., and Borg-Franck, M. (1992). Structure and expression of kin2, one of two cold- and ABA-induced genes of *Arabidopsis thaliana*. *Plant Mol. Biol.* 19, 689–692. doi: 10.1007/BF00026794
- Lambertucci, S., Orman, K. M., Dasgupta, S., Fisher, J. P., Gazal, S., Williamson, R. J., et al. (2019). Analysis of barley leaf epidermis and extrahaustorial proteomes during powdery mildew infection reveals that the PR5 thaumatin-like protein TLP5 is required for susceptibility towards *Blumeria graminis* f. sp. *hordei*. *Front. In Plant Sci.* 10, 1138. doi: 10.3389/fpls.2019.01138
- Lara, M. E. B., Garcia, M.-C. G., Fatima, T., Ehneß, R., Lee, T. K., Proels, R., et al. (2004). Extracellular invertase is an essential component of cytokinin-mediated delay of senescence. *Plant Cell* 16, 1276–1287. doi: 10.1105/tpc.018929
- Lebrasseur, N. D., Macintosh, G. C., Perez-Amador, M. A., Saitoh, M., and Green, P. J. (2002). Local and systemic wound-induction of RNase and nuclease activities in Arabidopsis: RNS1 as a marker for a JA-independent systemic signaling pathway. *Plant J.* 29, 393–403. doi: 10.1046/j.1365-313x.2002.01223.x
- Lee, S., Lee, E. J., Yang, E. J., Lee, J. E., Park, A. R., Song, W. H., et al. (2004). Proteomic identification of annexins, calcium-dependent membrane binding proteins that mediate osmotic stress and abscisic acid signal transduction in Arabidopsis. *Plant Cell* 16, 1378–1391. doi: 10.1105/tpc.021683
- Levesque-Tremblay, G., Pelloux, J., Braybrook, S. A., and Müller, K. (2015). Tuning of pectin methylesterification: consequences for cell wall biomechanics and development. *Planta* 242, 791–811. doi: 10.1007/s00425-015-2358-5
- Lippuner, V., Chou, I. T., Scott, S. V., Ettinger, W. F., Theg, S. M., and Gasser, C. S. (1994). Cloning and characterization of chloroplast and cytosolic forms of cyclophilin from *Arabidopsis thaliana*. *J. Biol. Chem.* 269, 7863–7868.
- Little, D., Gouhier-Darimont, C., Bruessow, F., and Reymond, P. (2007). Oviposition by pierid butterflies triggers defense responses in Arabidopsis. *Plant Physiol.* 143, 784–800. doi: 10.1104/pp.106.090837
- Liu, W. X., Zhang, F. C., Zhang, W. Z., Song, L. F., Wu, W. H., and Chen, Y. F. (2013). Arabidopsis Di19 functions as a transcription factor and modulates PR1, PR2, and PR5 expression in response to drought stress. *Mol. Plant* 6, 1487–1502. doi: 10.1093/mp/sst031
- Lohaus, G., Pennewiss, K., Sattelmacher, B., Hussmann, M., and Hermann Muehling, K. (2001). Is the infiltration-centrifugation technique appropriate for the isolation of apoplastic fluid? A critical evaluation with different plant species. *Physiol. Plant.* 111, 457–465. doi: 10.1034/j.1399-3054.2001.1110405.x
- Mammarella, N. D., Cheng, Z., Fu, Z. Q., Daudi, A., Bolwell, G. P., Dong, X., et al. (2015). Apoplastic peroxidases are required for salicylic acid-mediated defense against *Pseudomonas syringae*. *Phytochemistry* 112, 110–121. doi: 10.1016/j.phytochem.2014.07.010
- Mano, J., Nagata, M., Okamura, S., Shiraya, T., and Mitsui, T. (2014). Identification of oxidatively modified proteins in salt-stressed Arabidopsis: a carbonyl-targeted proteomics approach. *Plant Cell Physiol.* 55, 1233–1244. doi: 10.1093/pcp/pcu072
- Martínez, D. E., and Guaiamet, J. J. (2014). Senescence-related changes in the leaf apoplast. *J. Plant Growth Regul.* 33, 44–55. doi: 10.1007/s00344-013-9395-8
- Martínez-González, A. P., Ardila, H. D., Martínez-Peralta, S. T., Melgarejo-Muñoz, L., Castillejo-Sánchez, M., and Jorrin-Navo, J. V. (2018). What proteomic analysis of the apoplast tells us about plant-pathogen interactions. *Plant Pathol.* 67, 1647–1668. doi: 10.1111/ppa.12893
- Martínez, D. E., Borniego, M. L., Battchikova, N., Aro, E. M., Tyystjarvi, E., and Guaiamet, J. J. (2015). SASP, a Senescence-Associated Subtilisin Protease, is involved in reproductive development and determination of silique number in Arabidopsis. *J. Exp. Bot.* 66, 161–174. doi: 10.1093/jxb/eru409
- Masachis, S., Segorbe, D., Turrà, D., Leon-Ruiz, M., Fürst, U., El Ghalid, M., et al. (2016). A fungal pathogen secretes plant alkalizing peptides to increase infection. *Nat. Microbiol.* 1, 16043. doi: 10.1038/nmicrobiol.2016.43
- Mattsson, M., and Schjoerring, J. K. (2003). Senescence-induced changes in apoplastic and bulk tissue ammonia concentrations of ryegrass leaves. *New Phytol.* 160, 489–499. doi: 10.1046/j.1469-8137.2003.00902.x
- Megel, C., Hummel, G., Lalande, S., Ubrig, E., Cognat, V., Morelle, G., et al. (2019). Plant RNases T2, but not Dicer-like proteins, are major players of tRNA-derived fragments biogenesis. *Nucleic Acids Res.* 47, 941–952. doi: 10.1093/nar/gky1156
- Mishina, T. E., and Zeier, J. (2007). Pathogen-associated molecular pattern recognition rather than development of tissue necrosis contributes to bacterial induction of systemic acquired resistance in Arabidopsis. *Plant J.* 50, 500–513. doi: 10.1111/j.1365-313X.2007.03067.x
- Nardi, C. F., Villarreal, N. M., Rossi, F. R., Martinez, S., Martinez, G. A., and Civello, P. M. (2015). Overexpression of the carbohydrate binding module of strawberry expansin2 in *Arabidopsis thaliana* modifies plant growth and cell wall metabolism. *Plant Mol. Biol.* 88, 101–117. doi: 10.1007/s11103-015-0311-4
- Nguyen-Kim, H., San Clemente, H., Balliau, T., Zivy, M., Dunand, C., Albenne, C., et al. (2016). *Arabidopsis thaliana* root cell wall proteomics: Increasing the proteome coverage using a combinatorial peptide ligand library and description of unexpected Hyp in peroxidase amino acid sequences. *Proteomics* 16, 491–503. doi: 10.1002/pmic.201500129
- Noodén, L. D., Guaiamé, J. J., and John, I. (1997). Senescence mechanisms. *Physiol. Plant.* 101, 746–753. doi: 10.1111/j.1399-3054.1997.tb01059.x
- Nouchi, I., Hayashi, K., Hiradate, S., Ishikawa, S., Fukuoka, M., Chen, C. P., et al. (2012). Overcoming the difficulties in collecting apoplastic fluid from rice leaves by the infiltration-centrifugation method. *Plant Cell Physiol.* 53, 1659–1668. doi: 10.1093/pcp/pcs102
- O'Brien, J. A., Daudi, A., Finch, P., Butt, V. S., Whitelegge, J. P., Souda, P., et al. (2012). A peroxidase-dependent apoplastic oxidative burst in cultured Arabidopsis cells functions in MAMP-elicited defense. *Plant Physiol.* 158, 2013–2027. doi: 10.1104/pp.111.190140

- O'leary, B. M., Rico, A., McCraw, S., Fones, H. N., and Preston, G. M. (2014). The infiltration-centrifugation technique for extraction of apoplastic fluid from plant leaves using *Phaseolus vulgaris* as an example. *J. Vis. Exp.* e52113. doi: 10.3791/52113
- O'leary, B. M., Neale, H. C., Geilfus, C. M., Jackson, R. W., Arnold, D. L., and Preston, G. M. (2016). Early changes in apoplast composition associated with defence and disease in interactions between *Phaseolus vulgaris* and the halo blight pathogen *Pseudomonas syringae* pv. *phaseolicola*. *Plant Cell Environ.* 39, 2172–2184. doi: 10.1111/pce.12770
- Oda-Yamamizo, C., Mitsuda, N., Sakamoto, S., Ogawa, D., Ohme-Takagi, M., and Ohmiya, A. (2016). The NAC transcription factor ANAC046 is a positive regulator of chlorophyll degradation and senescence in *Arabidopsis* leaves. *Sci. Rep.* 6, 23609. doi: 10.1038/srep35125
- Otegui, M. S. (2018). Vacuolar degradation of chloroplast components: autophagy and beyond. *J. Exp. Bot.* 69, 741–750. doi: 10.1093/jxb/erx234
- Park, S.-W., Li, W., Viehhauser, A., He, B., Kim, S., Nilsson, A. K., et al. (2013). Cyclophilin 20-3 relays a 12-oxo-phytodienoic acid signal during stress responsive regulation of cellular redox homeostasis. *Proc. Natl. Acad. Sci.* 110, 9559–9564. doi: 10.1073/pnas.1218872110
- Petersen, T. N., Brunak, S., Von Heijne, G., and Nielsen, H. (2011). SignalP 4.0: discriminating signal peptides from transmembrane regions. *Nat. Methods* 8, 785–786. doi: 10.1038/nmeth1701
- Piofczyk, T., Jeena, G., and Pecinka, A. (2015). *Arabidopsis thaliana* natural variation reveals connections between UV radiation stress and plant pathogen-like defense responses. *Plant Physiol. Biochem.* 93, 34–43. doi: 10.1016/j.plaphy.2015.01.011
- Potter, S., Uknes, S., Lawton, K., Winter, A. M., Chandler, D., Dimairo, J., et al. (1993). Regulation of a hevein-like gene in *Arabidopsis*. *Mol. Plant-Microbe Interact.* 6, 680–685. doi: 10.1094/MPMI-6-680
- Provart, N. J., Gil, P., Chen, W., Han, B., Chang, H. S., Wang, X., et al. (2003). Gene expression phenotypes of *Arabidopsis* associated with sensitivity to low temperatures. *Plant Physiol.* 132, 893–906. doi: 10.1104/pp.103.021261
- Rascio, A., Platani, C., Di Fonzo, N., and Wittmer, G. (1992). Bound water in durum wheat under drought stress. *Plant Physiol.* 98, 908–912. doi: 10.1104/pp.98.3.908
- Rizhsky, L., Liang, H., Shuman, J., Shulaev, V., Davletova, S., and Mittler, R. (2004). When defense pathways collide. The response of *Arabidopsis* to a combination of drought and heat stress. *Plant Physiol.* 134, 1683–1696. doi: 10.1104/pp.103.033431
- Robinson, W. D., Carson, I., Ying, S., Ellis, K., and Plaxton, W. C. (2012). Eliminating the purple acid phosphatase AtPAP26 in *Arabidopsis thaliana* delays leaf senescence and impairs phosphorus remobilization. *New Phytol.* 196, 1024–1029. doi: 10.1111/nph.12006
- Rodríguez-Celma, J., Ceballos-Laita, L., Grusak, M. A., Abadía, J., and López-Millán, A.-F. (2016). Plant fluid proteomics: delving into the xylem sap, phloem sap and apoplastic fluid proteomes. *Biochim. Biophys. Acta* 1864, 991–1002. doi: 10.1016/j.bbapap.2016.03.014
- Rutter, B. D., and Innes, R. W. (2017). Extracellular vesicles isolated from the leaf apoplast carry stress-response proteins. *Plant Physiol.* 173, 728–741. doi: 10.1104/pp.16.01253
- Sävenstrand, H., Brosché, M., and Strid, A. (2004). Ultraviolet-B signalling: *Arabidopsis* brassinosteroid mutants are defective in UV-B regulated defence gene expression. *Plant Physiol. Biochem.* 42, 687–694. doi: 10.1016/j.plaphy.2004.06.011
- Sattelmacher, B., and Horst, W. J. (2007). *The apoplast of higher plants: compartment of storage, transport and reactions: the significance of the apoplast for the mineral nutrition of higher plants* (Dordrecht, The Netherlands: Springer Science & Business Media). doi: 10.1007/978-1-4020-5843-1
- Schippers, J. H., Schmidt, R., Wagstaff, C., and Jing, H. C. (2015). Living to die and dying to live: the survival strategy behind leaf senescence. *Plant Physiol.* 169, 914–930. doi: 10.1104/pp.15.00498
- Seo, P. J., Lee, A.-K., Xiang, F., and Park, C.-M. (2008). Molecular and functional profiling of *Arabidopsis* pathogenesis-related genes: insights into their roles in salt response of seed germination. *Plant Cell Physiol.* 49, 334–344. doi: 10.1093/pcp/pcn011
- Soares, J. R., Jose Tenorio De Melo, E., Da Cunha, M., Fernandes, K. V. S., Taveira, G. B., Da Silva Pereira, L., et al. (2017). Interaction between the plant ApDef1 defensin and *Saccharomyces cerevisiae* results in yeast death through a cell cycle- and caspase-dependent process occurring via uncontrolled oxidative stress. *Biochim. Biophys. Acta* 1861, 3429–3443. doi: 10.1016/j.bbagen.2016.09.005
- Song, W., Mentink, R. A., Henquet, M. G., Cordewener, J. H., Van Dijk, A. D., Bosch, D., et al. (2013). N-glycan occupancy of *Arabidopsis* N-glycoproteins. *J. Proteomics* 93, 343–355. doi: 10.1016/j.jprot.2013.07.032
- Suzuki, N., Rizhsky, L., Liang, H., Shuman, J., Shulaev, V., and Mittler, R. (2005). Enhanced tolerance to environmental stress in transgenic plants expressing the transcriptional coactivator multiprotein bridging factor 1c. *Plant Physiol.* 139, 1313–1322. doi: 10.1104/pp.105.070110
- Taira, M., Valtersson, U., Burkhardt, B., and Ludwig, R. A. (2004). *Arabidopsis thaliana* GLN2-encoded glutamine synthetase is dual targeted to leaf mitochondria and chloroplasts. *Plant Cell* 16, 2048–2058. doi: 10.1105/tpc.104.022046
- Tetlow, I., and Farrar, J. (1993). Apoplastic sugar concentration and pH in barley leaves infected with brown rust. *J. Exp. Bot.* 44, 929–936. doi: 10.1093/jxb/44.5.929
- Tran, H. T., and Plaxton, W. C. (2008). Proteomic analysis of alterations in the secretome of *Arabidopsis thaliana* suspension cells subjected to nutritional phosphate deficiency. *Proteomics* 8, 4317–4326. doi: 10.1002/pmic.200800292
- Tran, H. T., Qian, W., Hurley, B. A., She, Y. M., Wang, D., and Plaxton, W. C. (2010). Biochemical and molecular characterization of AtPAP12 and AtPAP26: the predominant purple acid phosphatase isozymes secreted by phosphate-starved *Arabidopsis thaliana*. *Plant Cell Environ.* 33, 1789–1803. doi: 10.1111/j.1365-3040.2010.02184.x
- Trusova, S. V., Chichkova, N. V., and Vartapetian, A. B. (2019). Sometimes they come back: endocytosis provides localization dynamics of a subtilase in cells committed to cell death. *J. Exp. Bot.* 70, 2003–2007. doi: 10.1093/jxb/erz014
- Tyree, M. (1976). Negative turgor pressure in plant cells: fact or fallacy? *Can. J. Bot.* 54, 2738–2746. doi: 10.1139/b76-294
- Uknes, S., Mauch-Mani, B., Moyer, M., Potter, S., Williams, S., Dincher, S., et al. (1992). Acquired resistance in *Arabidopsis*. *Plant Cell* 4, 645–656. doi: 10.1105/tpc.4.6.645
- Van Der Graaff, E., Schwacke, R., Schneider, A., Desimone, M., Flügge, U.-I., and Kunze, R. (2006). Transcription analysis of *Arabidopsis* membrane transporters and hormone pathways during developmental and induced leaf senescence. *Plant Physiol.* 141, 776–792. doi: 10.1104/pp.106.079293
- Van Loon, L., and Van Strien, E. (1999). The families of pathogenesis-related proteins, their activities, and comparative analysis of PR-1 type proteins. *Physiol. Mol. Plant Pathol.* 55, 85–97. doi: 10.1006/pmpp.19990213
- Velazhahan, R., Datta, S. K., and Muthukrishnan, S. (1999). “The PR-5 family: thaumatin-like proteins,” in *Pathogenesis-related proteins in plants*. Eds. S. K. Datta and S. Muthukrishnan (Boca Raton: CRC Press), 107–129.
- Wardlaw, I. F. (2005). Consideration of apoplastic water in plant organs: a reminder. *Funct. Plant Biol.* 32, 561–569. doi: 10.1071/FP04127
- Wei, C., and Lintilhac, P. M. (2007). Loss of stability: a new look at the physics of cell wall behavior during plant cell growth. *Plant Physiol.* 145, 763–772. doi: 10.1104/pp.107.101964
- Wei, H., Brunecky, R., Donohoe, B. S., Ding, S.-Y., Ciesielski, P. N., Yang, S., et al. (2015). Identifying the ionically bound cell wall and intracellular glycoside hydrolases in late growth stage *Arabidopsis* stems: implications for the genetic engineering of bioenergy crops. *Front. In Plant Sci.* 6, 315. doi: 10.3389/fpls.2015.00315
- Winter, D., Vinegar, B., Nahal, H., Ammar, R., Wilson, G. V., and Provart, N. J. (2007). An “Electronic Fluorescent Pictograph” browser for exploring and analyzing large-scale biological data sets. *PLoS One* 2, e718. doi: 10.1371/journal.pone.0000718
- Wu, Y., Yang, T., Song, Y., Zhang, X., Xu, S., Xue, G., et al. (2016). Metabolic regulation of ammonia emission in different senescence phenotypes of *Nicotiana tabacum*. *Biol. Plant.* 60, 190–194. doi: 10.1007/s10535-015-0556-4
- Zörb, C., Mühling, K. H., Kutschera, U., and Geilfus, C.-M. (2015). Salinity stiffens the epidermal cell walls of salt-stressed maize leaves: is the epidermis growth-restricting? *PLoS One* 10, e0118406. doi: 10.1371/journal.pone.0118406
- Zabaleta, E., Oropeza, A., Assad, N., Mandel, A., Salerno, G., and Herrera-Estrella, L. (1994). Antisense expression of chaperonin 60β in transgenic tobacco plants leads to abnormal phenotypes and altered distribution of photoassimilates. *Plant J.* 6, 425–432. doi: 10.1046/j.1365-313X.1994.06030425.x

- Zavaliev, R., Levy, A., Gera, A., and Epel, B. L. (2013). Subcellular dynamics and role of Arabidopsis beta-1,3-glucanases in cell-to-cell movement of tobamoviruses. *Mol. Plant Microbe Interact.* 26, 1016–1030. doi: 10.1094/MPMI-03-13-0062-R
- Zhang, L., Cheng, J., Sun, X., Zhao, T., Li, M., Wang, Q., et al. (2018). Overexpression of VaWRKY14 increases drought tolerance in Arabidopsis by modulating the expression of stress-related genes. *Plant Cell Rep.* 37, 1159–1172. doi: 10.1007/s00299-018-2302-9
- Zhao, J., Wang, J., An, L., Doerge, R. W., Chen, Z. J., Grau, C. R., et al. (2007). Analysis of gene expression profiles in response to *Sclerotinia sclerotiorum* in *Brassica napus*. *Planta* 227, 13–24. doi: 10.1007/s00425-007-0586-z
- Zhao, Y., Chan, Z., Gao, J., Xing, L., Cao, M., Yu, C., et al. (2016). ABA receptor PYL9 promotes drought resistance and leaf senescence. *Proc. Natl. Acad. Sci.* 113, 1949–1954. doi: 10.1073/pnas.1522840113
- Zhao, P., Zhang, F., Liu, D., Imani, J., Langen, G., and Kogel, K. H. (2017). Matrix metalloproteinases operate redundantly in Arabidopsis immunity against necrotrophic and biotrophic fungal pathogens. *PLoS One* 12, e0183577. doi: 10.1371/journal.pone.0183577
- Zhou, Q., Yu, Q., Wang, Z., Pan, Y., Lv, W., Zhu, L., et al. (2013). Knockdown of GDCH gene reveals reactive oxygen species-induced leaf senescence in rice. *Plant Cell Environ.* 36, 1476–1489. doi: 10.1111/pce.12078
- Ziemann, S., Linde, K., Lahrman, U., Acar, B., Kaschani, F., Colby, T., et al. (2018). An apoplastic peptide activates salicylic acid signalling in maize. *Nat. Plants* 4, 172–180. doi: 10.1038/s41477-018-0116-y

Conflict of Interest: The authors declare that the research was conducted in the absence of any commercial or financial relationships that could be construed as a potential conflict of interest.

Copyright © 2020 Borniego, Molina, Guiamét and Martínez. This is an open-access article distributed under the terms of the Creative Commons Attribution License (CC BY). The use, distribution or reproduction in other forums is permitted, provided the original author(s) and the copyright owner(s) are credited and that the original publication in this journal is cited, in accordance with accepted academic practice. No use, distribution or reproduction is permitted which does not comply with these terms.